Table 1
Primer sequences used for PCR amplification

Gene	Primer sequence (5′ → 3′)	Product size (bp)
Mouse CCL17	(F) TGC TTC TGG GGA CTT TTC TG (R) CCT TGG GTT TTT CAC CAA TC	242
Mouse CCL19	(F) GAA AGC CTT CCG CTA CCT TC (R) TGC TGT TGC CTT TGT TCT TG	164
Mouse CCL20	(F) CGA CTG TTG CCT CTC GTA CA (R) CAC CCA GTT CTG CTT TGG AT	157
Mouse CCL21	(F) CTG AGC CTC CTT AGC CTG GT (R) TCC TCT TGA GGG CTG TGT CT	381
Mouse CCL22	(F) TAT GGT GCC AAT GTG GAA GA (R) GCA GGA TTT TGA GGT CCA GA	102
Mouse CCL27	(F) CTC CCG CTG TTA CTG TTG CT (R) AGT TTT GCT GTT GGG GGT TT	331
Mouse XCL1	(F) ATG GGT TGT GGA AGG TGT G (R) GGG AAC AGT TTC AGC CAT GT	250
Mouse CX3CL1	(F) GCA GTG ACC GGA TCA TCT CT (R) GGC ACC AGG ACG TAT GAG TT	701
Human β-actin	(F) CCT TCC TGG GCA TGG AGT CCT G (R) GGA GCA ATG ATC TTG ATC TTC	202

cultivation, cells were washed and incubated with an assay medium (phenol red-free RPMI 1640 containing 0.5% bovine serum albumin and 20 mM Hepes, pH 7.4) for another 24 h. The resulting conditioned medium was collected, and its chemoattractant activity was measured by an in vitro chemotaxis assay across a polycarbonate membrane with 5-μm pores (Chemotaxicell-24; Kurabo, Osaka, Japan) using L1.2 transfectants expressing the specific receptor for chemokines. Recombinant chemokines corresponding to each specific receptor (mouse: CCL19, CCL20, CCL22, CCL27, XCL1, and CX3CL1) were purchased from DakoCytomation (Kyoto, Japan) and used as a positive control for cell migration. Migration was allowed for 2 h at 37 °C in a 5% CO_2 atmosphere. The migrated cells were lysed and quantitated using a PicoGreen dsDNA quantitation reagent (Invitrogen, Tokyo, Japan), and the migration activity was expressed in term of the percentage of the input cells calculated by the following formula: (% of input cells) = (the number of migrated cells)/(the number of cells placed in Chemotaxicell-24; 1×10^6 cells) × 100.

Evaluation of growth of chemokine gene-transduced tumor cells in immunocompetent mice. B16BL6, CT26, and OV-HM cells were transfected with each AdRGD at an MOI of 400, 50, and 10, respectively. After 24 h cultivation, the cells were harvested and washed three times with PBS, and then 2×10^5 transduced B16BL6 cells, 2×10^5 transduced CT26 cells, and 1×10^6 transduced OV-HM cells were intradermally inoculated into the flank of C57BL/6 mice, BALB/c mice, and B6C3F1 mice, respectively. The major and minor axes of the tumor were measured using microcalipers, and the tumor volume was calculated by the following formula: (tumor volume; mm^3) = (major axis; mm) × (minor axis; $mm)^2 \times 0.5236$ [20]. The mice were euthanized when one of the two measurements was greater than 15 mm. On day 60 after tumor inoculation, the tumor-free mice were judged as individuals that could achieve complete rejection. In some cases, the mice that could completely reject a primary tumor were rechallenged by intradermal injection into the flank with 1×10^6 parental or irrelevant tumor cells without chemokine gene-transduction at 3 months after the initial challenge.

Evaluation of growth and rejection ratio of chemokine gene-transduced B16BL6 cells in mice sensitized with melanoma-associated antigen. The immunization of mice with melanoma-associated antigen was performed by the administration of dendritic cells (DCs) transduced with the gp100 gene. The isolation, cultivation, and gene transduction procedures for C57BL/6 mouse bone marrow-derived DCs conformed to the methods previously described [21]. DCs transfected with Ad-RGD-gp100 at an MOI of 50 for 2 h were intradermally injected into the right flank of C57BL/6 mice at 5×10^5 cells/50 μl. At 1 week after the vaccination, 2×10^5 intact or transduced B16BL6 cells were inoculated into the left flank of the mice. The tumor growth and complete rejection were assessed as described above.

Results

Expression of chemokine mRNA and protein in cells transfected with AdRGD

In order to verify the vector performance of mouse chemokine gene-carried AdRGDs, we first examined

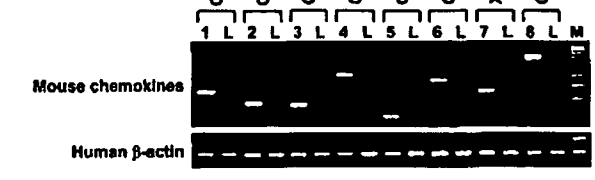

Fig. 1. RT-PCR analysis of chemokine mRNA expression in A549 cells transfected with each chemokine gene-carried AdRGD. PCR for mouse chemokine and human β-actin transcripts was performed on the same RT samples using each specific primer set (summarized in Table 1) to ensure the quality of the procedure. Lane L is negative control using AdRGD-LacZ-transfected A549 (LacZ/A549) cell-derived RT material. Lanes 1–8 represent CCL17/A549, CCL19/A549, CCL20/A549, CCL21/A549, CCL22/A549, CCL27/A549, XCL1/A549, and CX3CL1/A549, respectively. Lane M is a 100 bp molecular ruler.

mRNA expression in transfected cells by an RT-PCR analysis (Fig. 1). In this experiment, human lung carcinoma A549 cells were used instead of murine tumor cells to eliminate the influence of the expression of endogenous mouse chemokine. A549 cells transfected with AdRGD-CCL17, -CCL19, -CCL20, -CCL21, -CCL22, -CCL27, -XCL1, or -CX3CL1 expressed corresponding mouse chemokine mRNA, whereas no PCR products derived from the transcripts of the mouse chemokine gene were detected in AdRGD-LacZ-transfected A549 cells. Next, using in vitro chemotaxis assay, we investigated whether A549 cells transfected with each chemokine gene-carried AdRGD could secrete chemokine protein as a biologically active form into culture supernatants. As shown in Fig. 2, the culture supernatants of each chemokine gene-transduced A549 cell could induce greater migration of cells expressing the corresponding chemokine receptor than those of the intact A549 cells or the AdRGD-Luc-transfected A549 (Luc/A549) cells. The migration of parental L1.2 cells for chemokine receptor-transfectants was not observed in recombinant chemokine-added wells, and they were

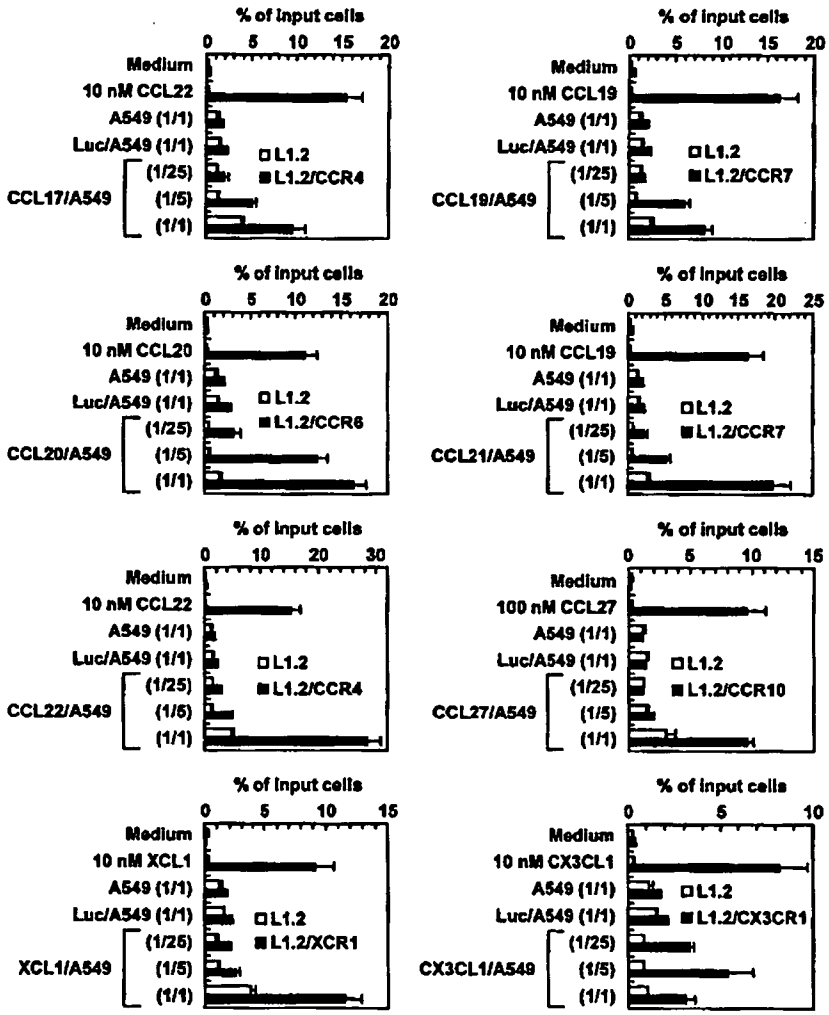

Fig. 2. Chemoattractant activity of culture supernatants of A549 cells transfected with each chemokine gene-carried AdRGD against the stable specific chemokine receptor-expressing cells. The culture supernatants of intact A549 cells, AdRGD-Luc-transfected A549 (Luc/A549) cells, and chemokine gene-transduced A549 cells were prepared and diluted with an assay medium. The fractional values with parentheses in each panel express the dilution factor. These samples and recombinant chemokines dissolved with the assay medium were added to a 24-well culture plate. Cells expressing specific receptors for CCL17 and CCL22 (L1.2/CCR4), CCL20 (L1.2/CCR6), CCL19 and CCL21 (L1.2/CCR7), CCL27 (L1.2/CCR10), XCL1 (L1.2/XCR1), or CX3CL1 (L1.2/CX3CR1) were suspended with the assay medium and placed in a Chemotaxicell-24 installed on each well at 1×10^6 cells. Likewise, parental L1.2 cells for these transfectants were prepared and added to Chemotaxicell-24. Cell migration was allowed for 2 h at 37 °C in a 5% CO_2 atmosphere. The cells that migrated to the lower well were lysed and quantitated using a PicoGreen dsDNA quantitation reagent. The data are expressed as means ± SE of the triplicate results.

maintained at low levels against the culture supernatants of intact A549, Luc/A549, and chemokine gene-transduced A549 cells. These results clearly demonstrated that all AdRGDs encoding each chemokine gene could deliver the concerned gene to target cells, and that transfected cells could secrete the chemokine protein which maintained original chemoattractant activity.

In vivo anti-tumor effect by transfection with chemokine-expressing AdRGD

B16BL6 and CT26 cells were each transfected with eight kinds of chemokine-expressing AdRGDs and AdRGD-Luc, as a control vector, at an MOI of 400 and 50, respectively. OV-HM cells were transfected with

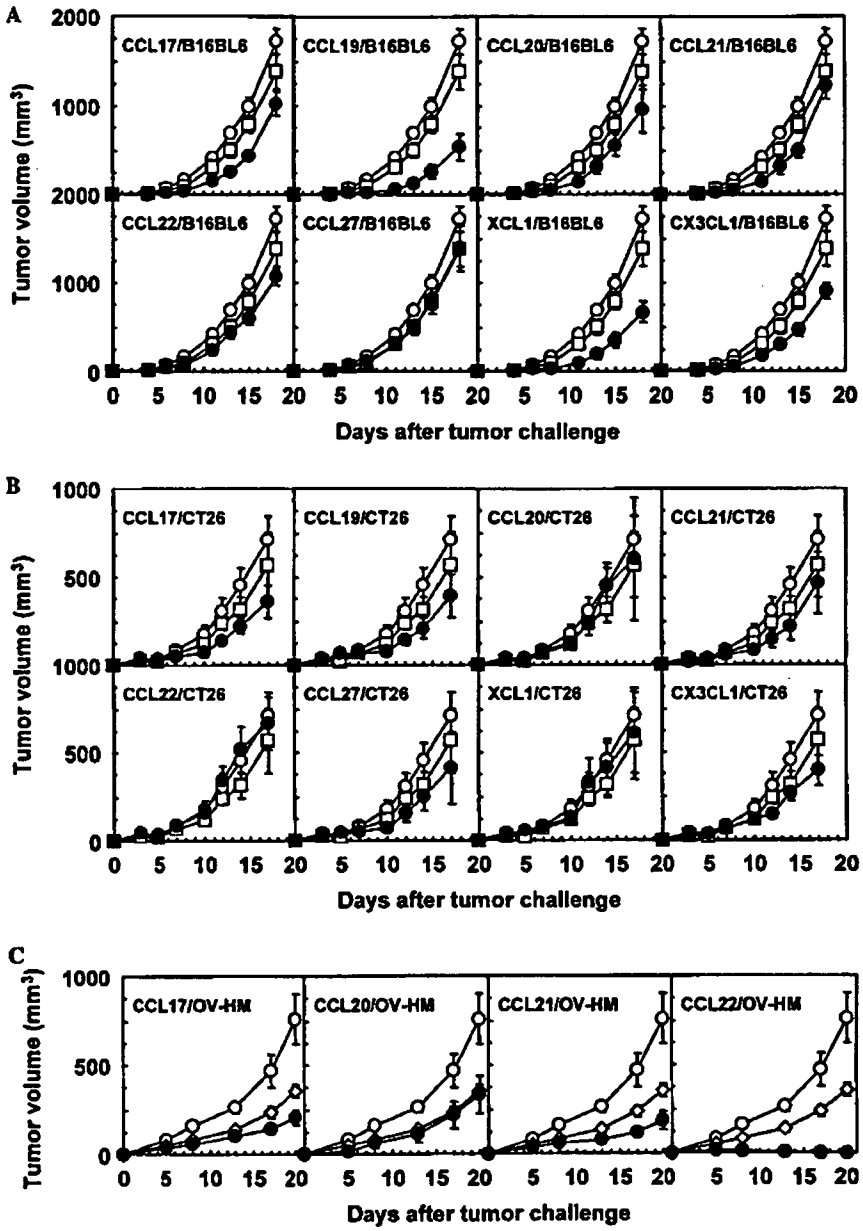

Fig. 3. In vivo growth of three kinds of murine tumor cells transduced with the chemokine gene. B16BL6 cells (A), CT26 cells (B), and OV-HM cells (C) were transfected with each chemokine-expressing AdRGD at an MOI of 400, 50, and 10, respectively, for 24 h. C57BL/6 mice, BALB/c mice, and B6C3F1 mice were intradermally injected in the flank with 2×10^5 transduced B16BL6 cells, 2×10^5 transduced CT26 cells, and 1×10^6 transduced OV-HM cells (●), respectively. Similarly, mice were inoculated with three kinds of intact tumor cells (○), AdRGD-Luc-transfected B16BL6 cells or CT26 cells (□), or AdRGD-Null-transfected OV-HM cells (◇), as control groups. The tumor volume was calculated after measuring the major and minor axes of the tumor at indicated points. Each point represents the mean ± SE of 6–10 mice. The data are representative of two independent experiments.

AdRGD-CCL17, -CCL20, -CCL21, -CCL22, or control AdRGD-Null at an MOI of 10. These transduced tumor cells were intradermally inoculated into H-2 haplotype-matched mice, and tumor growth was compared with that of intact tumors. As shown in Fig. 3, the tumorigenicity of B16BL6 and CT26 cells was hardly affected by transfection with the control vector, whereas OV-HM cells transfected with AdRGD-Null exhibited a slight delay of tumor growth as compared with intact OV-HM cells. Among 20 combinations of chemokine and tumor cells, an obvious tumor-suppressive effect was recognized in mice inoculated with CCL19/B16BL6, XCL1/B16BL6, or CCL22/OV-HM cells. In contrast, the in vivo growth of CCL27/B16BL6, CCL20/CT26, CCL22/CT26, XCL1/CT26, and CCL20/OV-HM cells was the same as that of the control vector-transfected cells, and only a slight delay of tumor growth was observed in five B16BL6 groups (CCL17, CCL20, CCL21, CCL22, and CX3CL1), five CT26 groups (CCL17, CCL19, CCL21, CCL27, and CX3CL1), and two OV-HM groups (CCL17 and CCL21). Importantly, CCL22/OV-HM cells not only demonstrated considerable retardation in tumor growth but were also completely rejected in 9 of 10 mice. In the rechallenge experiment, these cured mice were intradermally injected with 1×10^6 parental OV-HM cells or irrelevant B16BL6 cells at 3 months after the initial challenge. Five of six mice rechallenged with OV-HM cells remained tumor-free for more than 2 months, whereas rechallenging with B16BL6 cells perfectly developed palpable tumors in three additional mice within 2 weeks (data not shown). These results indicate the generation of long-term specific immunity against OV-HM tumor in mice that could once reject CCL22/OV-HM cells.

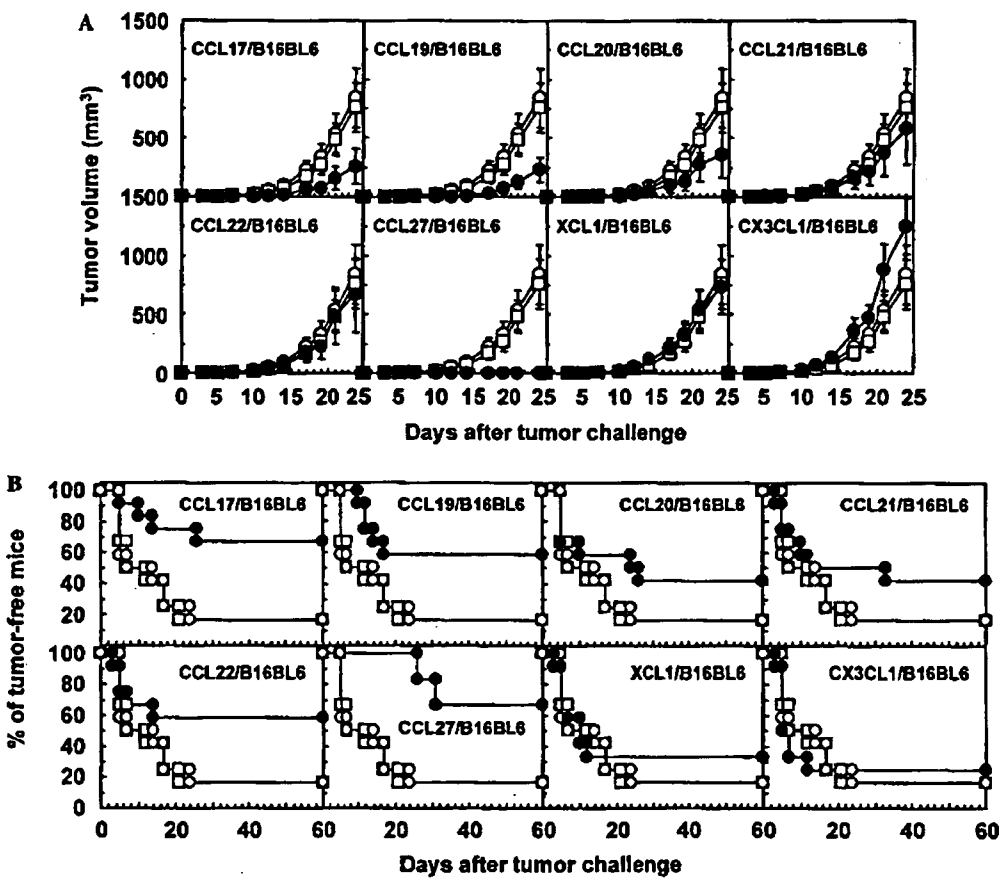

Fig. 4. Growth and rejection ratio of B16BL6 cells transduced with the chemokine gene in mice primed with melanoma-associated antigen. C57BL/6 mouse bone marrow-derived DCs were transfected with AdRGD-gp100 at an MOI of 50 for 2 h and they were intradermally injected into the right flank of syngeneic mice at 5×10^5 cells. At 1 week after the vaccination, these mice were intradermally inoculated in the left flank with 2×10^5 B16BL6 cells transfected with each chemokine-expressing AdRGD at an MOI of 400 for 24 h (●). Likewise, intact B16BL6 cells (○) or AdRGD-Luc-transfected B16BL6 cells (□) were inoculated in the gp100-primed mice, which were used as control groups. (A) The tumor volume was assessed three times per week. Each point represents the mean ± SE of results obtained from 12 mice. (B) Data are expressed in terms of the percentage of mice without visible tumor against the total mice tested in each group.

Growth and rejection ratio of chemokine gene-transfected B16BL6 cells in gp100-primed mice

For the purpose of examining the influence of chemokine against tumor growth in hosts specifically sensitized with tumor-associated antigen, B16BL6 cells transfected with chemokine-expressing AdRGD were inoculated into mice that were vaccinated with DCs presenting gp100, one of the identified melanoma-associated antigens. As shown in Fig. 4A, CCL17-, CCL19-, or CCL27-transfection was very effective for tumor growth suppression in gp100-primed mice, whereas AdRGD-Luc-transfected B16BL6 cells did not show any difference in tumor growth as compared with intact cells. A remarkable enhancement was observed in the complete rejection ratio at 2 months after tumor inoculation in the CCL22-transfected group as well as in the CCL17, CCL19, and CCL27 groups (Fig. 4B). Also, transfection with AdRGD-CCL20 or -CCL21 moderately improved the rejection ratio of B16BL6 cells in gp100-primed mice. XCL1 did not show a notable difference in both the growth and the rejection ratio of B16BL6 cells as compared with the control groups, and CX3CL1-transfected cells showed a tendency to promote tumor growth as compared with the intact B16BL6 cells.

Discussion

The application of chemokines to cancer immunotherapy has recently attracted great attention, because of their chemoattractant activity for a variety of immune cells as well as the angiostatic activity of some chemokines such as CXCL9 and CXCL10. In addition, it has been known that some tumor cells express a lower level of chemokines than normal cells [22]. Therefore, we may obtain novel cancer gene immunotherapy capable of demonstrating an excellent therapeutic effect, if a specific chemokine is adequately expressed at a local tumor site by gene transduction. The tumor-suppressive activity of several chemokines was observed in actuality in various experimental tumor models using the in vitro transfection method [8,23–27]. We also previously demonstrated that a CC family chemokine, CCL27, could suppress OV-HM tumor growth via transfection into the tumor cells due to the local recruitment of T cells and natural killer (NK) cell, whereas the transfection of CX3CL1 did not show a significant effect [19]. However, there are few reports comparing the antitumor activity of a specific chemokine between distinct tumor models.

Thus, we screened the potential anti-tumor activity of CCL17, CCL19, CCL20, CCL21, CCL22, CCL27, XCL1, and CX3CL1 in three murine tumor models by in vitro transfection. In order to efficiently transduce the chemokine gene into tumor cells, we constructed the AdRGDs carrying an expression cassette containing each murine chemokine cDNA by an improved in vitro ligation method. AdRGD can enhance gene transduction efficiency against a variety of tumor cells as compared with conventional Ad because of the expression of the RGD sequence, the αv-integrin-targeting peptide, at the HI-loop in their fiber knob [11–13]. Moreover, the improved in vitro ligation method enables speedy construction of a series of AdRGDs for screening by easy insertion of the expression cassette for the concerned gene into E1-deletion site [15,16]. With respect to the RT-PCR analysis and in vitro chemotaxis assay, transfection using our eight AdRGDs encoding the chemokine gene allowed tumor cells to express each corresponding chemokine mRNA and secrete a specific chemokine protein in a biologically active form (Figs. 1 and 2). Murine B16BL6 melanoma, murine CT26 colon carcinoma, and murine OV-HM ovarian carcinoma cells were transfected with chemokine-expressing AdRGDs at the MOI, which was suitable for adequately introducing a reporter gene into each tumor cell in preliminary examinations. To address the possibility of growth suppression depending on the cytotoxicity by AdRGD itself or secreted chemokine, we evaluated the viability of tumor cells transfected with each AdRGD at 48 h after transfection by MTT assay. The in vitro growth of the transfected cells was essentially identical to that of the intact cells with the exception of the OV-HM cells transduced with AdRGD-CCL19 or -XCL1 (data not shown). Therefore, CCL19 and XCL1 were excluded from the in vivo experiment using OV-HM cells.

Although a slight delay in tumor growth was observed in most of the combinations of tumor cells and chemokines, only CCL19/B16BL6, XCL1/B16BL6, and CCL22/OV-HM cells demonstrated a notable tumor-suppressive activity in immunocompetent mice as compared with the control vector-transfected cells (Fig. 3). In particular, CCL22-transfection was highly efficacious for the repression of OV-HM tumor growth, since complete rejection was observed in 9 of 10 mice. Furthermore, five of six cured mice could resist rechallenge with parental OV-HM cells, indicating the generation of a long-term tumor-specific immunity by rejection of CCL22/OV-HM cells. CCL22 exhibits a strong chemoattractant activity for a variety of immune cells including T cells, NK cells, and DCs. Guo et al. [28] also reported that the intratumoral injection of conventional Ad encoding human CCL22 resulted in a marked tumor regression in a murine 3LL lung carcinoma model with significant cytotoxic T lymphocyte (CTL) activity. However, CCL22-transfection did not show an antitumor effect in both B16BL6 and CT26 cells, and the chemokine that could demonstrate an obvious suppressive effect common to tumor cells of all three kinds was not found even if the results of CCL27/OV-HM and

CX3CL1/OV-HM cells, which were examined in our previous work [19], were included. In addition, some chemokines such as CCL17, CCL20, CCL21, and CX3CL1 failed to induce a notable suppressive effect against all three kinds of tumors although their chemoattractant activity for immune cells was reported. These complicated phenomena suggest that the anti-tumor effect via chemokine expression might be affected by several factors, for example, (1) the immunogenicity of the tumor cells, (2) the quantity and population ratio of the immune cells accumulated in tumor tissue, and (3) the activation state and deviation of the immune system in host.

We considered that not only the accumulation but also the activation of immune cells in tumor tissue is very important in cancer immunotherapy using chemokines, because several approaches that combined chemokines with cytokines or costimulatory molecules resulted in the synergic enhancement of anti-tumor activity as compared with the application of chemokine alone [29–32]. DCs, unique antigen-presenting cells capable of priming and stimulating naive T cells, not only play a critical role in establishing antigen-specific adaptive immune responses but also regulate the innate immune system [33–35]. Because of these properties, DCs loaded with tumor-associated antigen are ideal for generating a primary immune response against cancer as "nature's adjuvant" [33,36]. We previously reported that the vaccination of DCs transfected with gene coding gp100, one of the melanoma-associated antigens, by AdRGD could induce anti-B16BL6 tumor immunity based on increasing cytotoxic activities of NK cells and gp100-specific CTLs [21]. When chemokine-transfected B16BL6 cells were inoculated into mice vaccinated with gp100-expressing DCs, CCL17, CCL19, CCL22, and CCL27 could promote resistance to tumor formation (Fig. 4). Upon comparing the outcomes in Figs. 3A and 4, CCL19 demonstrated B16BL6 tumor-suppressive activity in both intact and gp100-primed mice, whereas the enhancement of the anti-tumor effect by CCL17, CCL22, or CCL27 was observed only in gp100-primed mice. Surprisingly, the anti-tumor activity of XCL1 detected in intact mice was lost in gp100-primed mice, and the CX3CL1/B16BL6 tumor grew more rapidly than the control tumor in gp100-primed mice. We speculated that the weak anti-B16BL6 tumor activity of XCL1 or CX3CL1 was masked by vaccine efficacy of gp100-expressing DCs, and that the angiogenic activity of CX3CL1 [37] might be emphasized in a tumor-specifically sensitized host.

Collectively, our data suggested that the tumor-suppressive activity of chemokine was greatly influenced by the kind of tumors and the activation state of the immune cells, and that a search for an effective chemokine for cancer immunotherapy should be performed in an experimental model that can reflect clinical status, including the immunogenicity of tumors, the state of the host's immune system, and the combination of other treatments, as much as possible.

Acknowledgments

We are grateful to Dr. Nicholas P. Restifo (National Cancer Institute, Bethesda, MD, USA) for providing the CT26 cells, and to Dr. Hiromi Fujiwara (School of Medicine, Osaka University, Osaka, Japan) for providing the OV-HM cells. This study was supported in part by the Research on Health Sciences focusing on Drug Innovation from The Japan Health Sciences Foundation; by grants from the Bioventure Development Program of the Ministry of Education, Culture, Sports, Science and Technology of Japan; by the Science Research Promotion Fund of the Japan Private School Promotion Foundation; by Grants-in-Aid for Scientific Research (C) from the Ministry of Education, Culture, Sports, Science and Technology of Japan; and by grants from the Ministry of Health and Welfare in Japan.

References

[1] A. Zlotnik, O. Yoshie, Chemokines: a new classification system and their role in immunity, Immunity 12 (2000) 121–127.
[2] O. Yoshie, T. Imai, H. Nomiyama, Chemokines in immunity, Adv. Immunol. 78 (2001) 57–110.
[3] B. Homey, A. Muller, A. Zlotnik, Chemokines: agents for the immunotherapy of cancer?, Nat. Rev. Immunol. 2 (2002) 175–184.
[4] S. Sharma, M. Stolina, J. Luo, R.M. Strieter, M. Burdick, L.X. Zhu, R.K. Batra, S.M. Dubinett, Secondary lymphoid tissue chemokine mediates T cell-dependent antitumor responses in vivo, J. Immunol. 164 (2000) 4558–4563.
[5] T. Fushimi, A. Kojima, M.A. Moore, R.G. Crystal, Macrophage inflammatory protein 3α transgene attracts dendritic cells to established murine tumors and suppresses tumor growth, J. Clin. Invest. 105 (2000) 1383–1393.
[6] S.E. Braun, K. Chen, R.G. Foster, C.H. Kim, R. Hromas, M.H. Kaplan, H.E. Broxmeyer, K. Cornetta, The CC chemokine CKβ-11/MIP-3β/ELC/Exodus 3 mediates tumor rejection of murine breast cancer cells through NK cells, J. Immunol. 164 (2000) 4025–4031.
[7] T. Miyata, S. Yamamoto, K. Sakamoto, R. Morishita, Y. Kaneda, Novel immunotherapy for peritoneal dissemination of murine colon cancer with macrophage inflammatory protein-1β mediated by a tumor-specific vector, HVJ cationic liposomes, Cancer Gene Ther. 8 (2001) 852–860.
[8] J. Guo, M. Zhang, B. Wang, Z. Yuan, Z. Guo, T. Chen, Y. Yu, Z. Qin, X. Cao, Fractalkine transgene induces T-cell-dependent antitumor immunity through chemoattraction and activation of dendritic cells, Int. J. Cancer 103 (2003) 212–220.
[9] K.F. Kozarsky, J.M. Wilson, Gene therapy: adenovirus vectors, Curr. Opin. Genet. Dev. 3 (1993) 499–503.
[10] M.A. Kay, S.L. Woo, Gene therapy for metabolic disorders, Trends Genet. 19 (1994) 253–257.
[11] H. Mizuguchi, N. Koizumi, T. Hosono, N. Utoguchi, Y. Watanabe, M.A. Kay, T. Hayakawa, A simplified system for constructing recombinant adenoviral vectors containing heterologous peptides in the HI loop of their fiber knob, Gene Ther. 8 (2001) 730–735.
[12] N. Koizumi, H. Mizuguchi, T. Hosono, A. Ishii-Watabe, E. Uchida, N. Utoguchi, Y. Watanabe, T. Hayakawa, Efficient gene transfer by fiber-mutant adenoviral vectors containing RGD peptide, Biochim. Biophys. Acta 1568 (2001) 13–20.

[13] Y. Okada, N. Okada, S. Nakagawa, H. Mizuguchi, K. Takahashi, N. Mizuno, T. Fujita, A. Yamamoto, T. Hayakawa, T. Mayumi, Tumor necrosis factor α-gene therapy for an established murine melanoma using RGD (Arg-Gly-Asp) fiber-mutant adenovirus vectors, Jpn. J. Cancer Res. 93 (2002) 436–444.
[14] H. Nomiyama, K. Hieshima, T. Nakayama, T. Sakaguchi, R. Fujisawa, S. Tanase, H. Nishiura, K. Matsuno, H. Takamori, Y. Tabira, T. Yamamoto, R. Miura, O. Yoshie, Human CC chemokine liver-expressed chemokine/CCL16 is a functional ligand for CCR1, CCR2 and CCR5, and constitutively expressed by hepatocytes, Int. Immunol. 13 (2001) 1021–1029.
[15] H. Mizuguchi, M.A. Kay, Efficient construction of a recombinant adenovirus vector by an improved in vitro ligation method, Hum. Gene Ther. 9 (1998) 2577–2583.
[16] H. Mizuguchi, M.A. Kay, A simple method for constructing E1- and E1/E4-deleted recombinant adenoviral vectors, Hum. Gene Ther. 10 (1999) 2013–2017.
[17] N. Okada, Y. Tsukada, S. Nakagawa, H. Mizuguchi, K. Mori, T. Saito, T. Fujita, A. Yamamoto, T. Hayakawa, T. Mayumi, Efficient gene delivery into dendritic cells by fiber-mutant adenovirus vectors, Biochem. Biophys. Res. Commun. 282 (2001) 173–179.
[18] N. Okada, Y. Masunaga, Y. Okada, S. Iiyama, N. Mori, T. Tsuda, A. Matsubara, H. Mizuguchi, T. Hayakawa, T. Fujita, A. Yamamoto, Gene transduction efficiency and maturation status in mouse bone marrow-derived dendritic cells infected with conventional or RGD fiber-mutant adenovirus vectors, Cancer Gene Ther. 10 (2003) 421–431.
[19] J.Q. Gao, Y. Tsuda, K. Katayama, T. Nakayama, Y. Hatanaka, Y. Tani, H. Mizuguchi, T. Hayakawa, O. Yoshie, Y. Tsutsumi, T. Mayumi, S. Nakagawa, Antitumor effect by interleukin-11 receptor α-locus chemokine/CCL27, introduced into tumor cells through a recombinant adenovirus vector, Cancer Res. 63 (2003) 4420–4425.
[20] P. Janik, P. Briand, N.R. Hartmann, The effect of estrone–progesterone treatment on cell proliferation kinetics of hormone-dependent GR mouse mammary tumours, Cancer Res. 35 (1975) 3698–3704.
[21] N. Okada, Y. Masunaga, Y. Okada, H. Mizuguchi, S. Iiyama, N. Mori, A. Sasaki, S. Nakagawa, T. Mayumi, T. Hayakawa, T. Fujita, A. Yamamoto, Dendritic cells transduced with gp100 gene by RGD fiber-mutant adenovirus vectors are highly efficacious in generating anti-B16BL6 melanoma immunity in mice, Gene Ther. 10 (2003) 1891–1902.
[22] F. Paillard, Cytokine and chemokine: a stimulating couple, Hum. Gene Ther. 10 (1999) 695–696.
[23] J. Laning, H. Kawasaki, E. Tanaka, Y. Luo, M.E. Dorf, Inhibition of in vivo tumor growth by the β chemokine, TCA3, J. Immunol. 153 (1994) 4625–4635.
[24] K. Hirose, M. Hakozaki, Y. Nyunoya, Y. Kobayashi, K. Matsushita, T. Takenouchi, A. Mikata, N. Mukaida, K. Matsushima, Chemokine gene transfection into tumour cells reduced tumorigenicity in nude mice in association with neutrophilic infiltration, Br. J. Cancer 72 (1995) 708–714.
[25] J.J. Mule, M. Custer, B. Averbook, J.C. Yang, J.S. Weber, D.V. Goeddel, S.A. Rosenberg, T.J. Schall, RANTES secretion by gene-modified tumor cells results in loss of tumorigenicity in vivo: role of immune cell subpopulations, Hum. Gene Ther. 7 (1996) 1545–1553.
[26] E. Nakashima, A. Oya, Y. Kubota, N. Kanada, R. Matsushita, K. Takeda, F. Ichimura, K. Kuno, N. Mukaida, K. Hirose, I. Nakanishi, T. Ujiie, K. Matsushima, A candidate for cancer gene therapy: MIP-1α gene transfer to an adenocarcinoma cell line reduced tumorigenicity and induced protective immunity in immunocompetent mice, Pharm. Res. 13 (1996) 1896–1901.
[27] M. Maric, Y. Liu, Strong cytotoxic T lymphocyte responses to a macrophage inflammatory protein 1α-expressing tumor: linkage between inflammation and specific immunity, Cancer Res. 59 (1999) 5549–5553.
[28] J. Guo, B. Wang, M. Zhang, T. Chen, Y. Yu, E. Regulier, H.E. Homann, Z. Qin, D.W. Ju, X. Cao, Macrophage-derived chemokine gene transfer results in tumor regression in murine lung carcinoma model through efficient induction of antitumor immunity, Gene Ther. 9 (2002) 793–803.
[29] P.C. Emtage, Y. Wan, M. Hitt, F.L. Graham, W.J. Muller, A. Zlotnik, J. Gauldie, Adenoviral vectors expressing lymphotactin and interleukin 2 or lymphotactin and interleukin 12 synergize to facilitate tumor regression in murine breast cancer models, Hum. Gene Ther. 10 (1999) 697–709.
[30] I. Narvaiza, G. Mazzolini, M. Barajas, M. Duarte, M. Zaratiegui, C. Qian, I. Melero, J. Prieto, Intratumoral coinjection of two adenoviruses, one encoding the chemokine IFN-γ-inducible protein-10 and another encoding IL-12, results in marked antitumoral synergy, J. Immunol. 164 (2000) 3112–3122.
[31] J.M. Ruehlmann, R. Xiang, A.G. Niethammer, Y. Ba, U. Pertl, C.S. Dolman, S.D. Gillies, R.A. Reisfeld, MIG (CXCL9) chemokine gene therapy combines with antibody-cytokine fusion protein to suppress growth and dissemination of murine colon carcinoma, Cancer Res. 61 (2001) 8498–8503.
[32] K.A. Tolba, W.J. Bowers, J. Muller, V. Housekneckt, R.E. Giuliano, H.J. Federoff, J.D. Rosenblatt, Herpes simplex virus (HSV) amplicon-mediated codelivery of secondary lymphoid tissue chemokine and CD40L results in augmented antitumor activity, Cancer Res. 62 (2002) 6545–6551.
[33] R.M. Steinman, Dendritic cells and immune-based therapies, Exp. Hematol. 24 (1996) 859–862.
[34] J. Banchereau, R.M. Steinman, Dendritic cells and the control of immunity, Nature 392 (1998) 245–252.
[35] F. Granucci, I. Zanoni, S. Feau, P. Ricciardi-Castagnoli, Dendritic cell regulation of immune responses: a new role for interleukin 2 at the intersection of innate and adaptive immunity, EMBO J. 22 (2003) 2546–2551.
[36] L. Fong, E.G. Engleman, Dendritic cells in cancer immunotherapy, Annu. Rev. Immunol. 18 (2000) 245–273.
[37] M.V. Volin, J.M. Woods, M.A. Amin, M.A. Connors, L.A. Harlow, A.E. Koch, Fractalkine: a novel angiogenic chemokine in rheumatoid arthritis, Am. J. Pathol. 159 (2001) 1521–1530.

Department of Biopharmaceutics[1], Graduate School of Pharmaceutical Sciences, Osaka University, Japan; Department of Pharmaceutics[2], School of Pharmaceutical Sciences, Zhejiang University, P.R. China; Division of Cellular and Gene Therapy Products[3], National Institute of Health Sciences, Japan

High gene expression of the mutant adenovirus vector, both *in vitro* and *in vivo*, with the insertion of integrin-targeting peptide into the fiber

J.Q. Gao[1,2], S. Inoue[1], Y. Tsukada[1], K. Katayama[1], Y. Eto[1], S. Kurachi[1], H. Mizuguchi[3], T. Hayakawa[3], Y. Tsutsumi[1], T. Mayumi[1], S. Nakagawa[1]

Received December 9, 2003, accepted February 25, 2004

Shinsaku Nakagawa, Ph.D Yamadaoka 1–6, 565–0871 Suita city, Osaka, Japan
hakagawa@phs.osaka-u.ac.jp

Pharmazie 59: 571–572 (2004)

In the present study, a first-generation adenovirus (Ad) vector was modified with the RGD peptide inserted into the fiber. The insertion of an integrin-targeting sequence into the Ad vector notably enhanced the luciferase expression in the Coxsackie virus and Adenovirus Receptor-deficient A2058 and B16BL6 melanoma cells. The results of an *in vivo* study with tumor-bearing mice also showed that Ad-RGD-Luc had enhanced gene expression in many organs and in the B16BL6 tumor compared to that induced by a conventional Ad vector after intravenous injection.

Adenovirus (Ad) vectors are widely used as carriers for gene therapy, both *in vitro* and *in vivo* (Asaoka et al. 2000; Gao et al. 2003; Gao et al. 2004). Recombinant Ad vectors can produce large amounts of gene products in a variety of dividing and nondividing cells. It has been reported that the initial process of Ad infection involves at least two sequential steps.

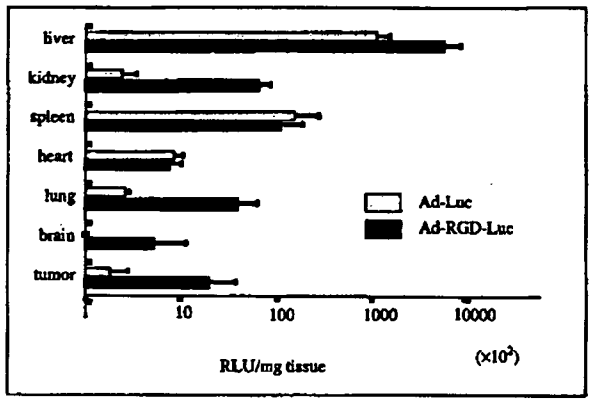

Fig. 2: Luciferase activity in organs after i.v. injection of Ad-Luc and Ad-RGD-Luc. The C57BL/6 mice were intradermally inoculated with 2×10^5 B16BL6 melanoma cells. After six days, 2×10^9 viral particles/mouse of Ad-Luc or Ad-RGD-Luc were injected into tail vein, respectively and the organs were harvested after 48 h. Then luciferase activity in organ homogenates was measured. Data are presented as the mean ± SD of relative light units (RLU)/mg tissue determined from four mice

The first step is the attachment of the virus to the cell surface, which occurs by binding of the fiber knob to the Coxsackie virus and Adenovirus Receptor (CAR) (Bergelson et al. 1997; Tomko et al. 1997). Following this, in the second step, the interaction between the RGD motif of the penton base with αv integrins, the secondary host-cell receptors, facilitates internalization by receptor-mediated endocytosis (Wickham et al. 1993; 1994). In other words, if the surface of host cells lack CAR, it is difficult to obtain an efficient gene transfer into those cells using a conventional Ad vector. For overcoming the low gene expression in CAR negative cells through Ad vectors, we developed a fiber-mutant Ad vector with an integrin-targeting RGD peptide by a simple *in vitro* method (Mizuguchi et al. 2001a). We anticipated that the fiber-mutant Ad system might target αv integrins during the first attachment to host cells. Therefore, this fiber-mutant system is an intriguing strategy for altering Ad tropism to enable efficient gene transduction into cells expressing little or no CAR. In the present study, we evaluated gene expression in A2058 human melanoma cells and B16BL6 mouse melanoma cells that are deficient in CAR and express ade-

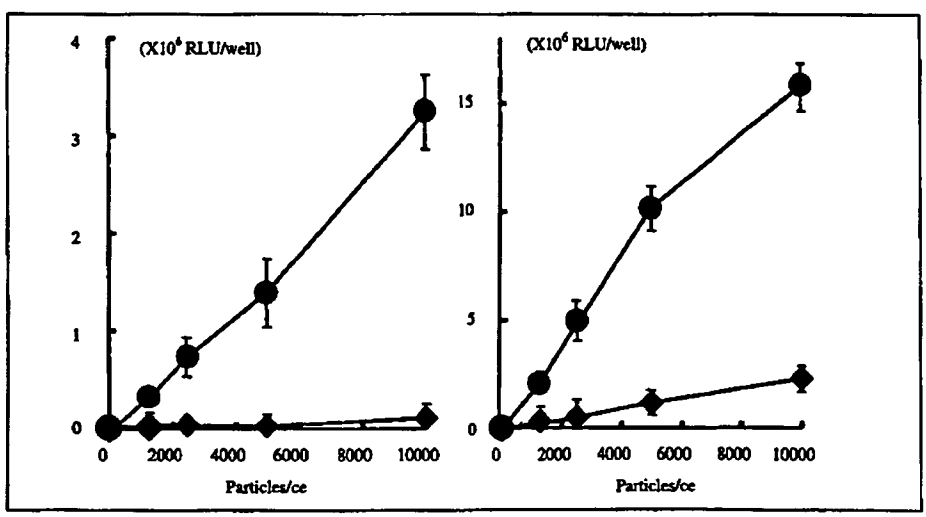

Fig. 1:
Luciferase expression of Ad-Luc or Ad-RGD-Luc infected A2058 and B16BL6 melanoma cells. A2058 cells (right) and B16BL6 cells (left) were transduced with Ad-Luc (◆) or Ad-RGD-Luc (●) respectively at the indicated viral particles/cell for 48 h. Subsequently, the cells were washed, collected, and their luciferase activity was measured. Data are presented as the mean ± SD of relative light units (RLU)/well determined from the three experiments

quate levels of αv integrins, which was confirmed by RT-PCR (data not shown). As shown in Fig. 1, A2058 cells and B16BL6 cells infected using Ad-RGD carrying the luciferase gene induced significantly enhanced gene expression compared to that induced by the Ad-Luc.

Subsequently, the gene expression of Ad-RGD was evaluated *in vivo*. Ad-RGD or the conventional Ad encoding luciferase gene was injected intravenously in tumor-bearing mice and the luciferase activity in each organ was measured. After insertion of the RGD peptide into the HI loop of the fiber, the Ad-RGD showed a significantly increased luciferase activity compared to that induced by a conventional Ad vector in liver, lung, brain, and B16BL6 tumor, while it showed almost similar gene expression in spleen and heart (Fig. 2). Hence, the enhanced gene transfer in tissues, especially in brain and tumor makes this vector a useful and powerful carrier for efficient gene transduction and gene therapy.

Experimental

1. Cell lines and animals

B16BL6 mouse melanoma cells were maintained in Minimal Essential Medium (MEM) supplemented with 7.5% heat-inactivated Fetal Bovine Serum (FBS). The human embryonic kidney (HEK) 293 cells and A2058 human melanoma cells were cultured in DMEM supplemented with 10% FBS. All the cell lines were cultured at 37 °C in a humidified atmosphere with 5% CO_2. The C57BL/6 female mice (4 weeks old) were purchased from SLC Inc. (Shizuoka, Japan). All the experimental procedures were in accordance with the Osaka University guidelines for the welfare of animals in experimental neoplasia.

2. Procedures

2.1. Construction of adenovirus vectors encoding RGD peptide in the fiber

The replication-deficient adenovirus vectors used in this study were constructed from the adenovirus serotype 5 backbone with deletions of E1 and E3 and the expression cassette in the E1 region (Mizuguchi et al. 2001a). The integrin-targeting RGD sequence was inserted into the HI loop of the fiber knob using the two-step method. The fiber-mutant adenovirus vector, Ad-RGD-Luc carrying the luciferase gene under the control of the cytomegalovirus (CMV) promoter, was constructed by an improved *in vitro* ligation method as described previously (Mizuguchi and Kay 1998). A conventional vector encoding luciferase gene (Ad-Luc) was also developed. The Ad vectors were propagated in HEK 293 cells and purified by cesium chloride gradient ultracentrifugation, and their titer was determined by plaque-forming assay.

2.2. Gene expression with Ad-RGD-Luc or conventional Ad-Luc in vitro

The A2058 human melanoma cells and B16BL6 mouse melanoma cells were infected with Ad-Luc or Ad-RGD-Luc at 1250, 2500, 5000, and 10000 viral particles/cell for 48 h. Subsequently, the cells were washed, collected, and their luciferase activity was measured using the Luciferase Assay System (Promega, USA) and Microlumat Plus LB96 (Perkin Elmer, USA) after the cells were lysed with the Luciferase Cell Culture Lysis (Promega, USA) according to the manufacturer's instruction.

2.3. Gene expression with Ad-RGD-Luc or conventional Ad-Luc in vivo

The C57BL/6 mice were intradermally inoculated with 2×10^5 B16BL6 melanoma cells. After 6 days, 2×10^9 viral particles/mouse of Ad-Luc or Ad-RGD-Luc were injected into the tail vein and the organs were harvested after 2 days. Subsequently, the luciferase activity in organ homogenates was measured using the method described in section 2.2.

References

Asaoka K, Tada M, Sawamura Y et al. (2000) Dependence of efficient adenoviral gene delivery in malignant glioma cells on the expression levels of the Coxsackievirus and adenovirus receptor. J Neurosurg 92: 1002–1008.

Bergelson JM, Cunningham JA, Droguett G et al. (1997) Isolation of a common receptor for Coxsackie B viruses and adenoviruses 2 and 5. Science. 275: 1320–1323.

Gao JQ, Tsuda Y, Katayama K et al. (2003) Anti-tumor effect by interleukin-11 receptor alpha-locus chemokine/CCL27, introduced into tumor cells through a recombinant adenovirus vector. Cancer Res 63: 4420–4425.

Gao JQ, Alexandre LS, Tsuda Y et al. (2004) Tumor-suppressive activities by chemokines introduced into OV-HM cells using fiber-mutant adenovirus vectors. Pharmazie 59: 238–239.

Mizuguchi H, Koizumi N, Hosono T et al. (2001a) A simplified system for constructing recombinant adenoviral vectors containing heterologous peptides in the HI loop of their fiber knob. Gene Ther 8: 730–735.

Mizuguchi H, Kay MA, Hayakawa T (2001b) *In vitro* ligation-based cloning of foreign DNAs into the E3 and E1 deletion regions for generation of recombinant adenovirus vectors. Biotechniques 30: 1112–1114.

Mizuguchi H, Kay MA (1998) Efficient construction of a recombinant adenovirus vector by an improved *in vitro* ligation method. Hum Gene Ther 9: 2577–2583.

Tomko RP, Xu R Philipson L (1997) HCAR and MCAR: the human and mouse cellular receptors for subgroup C adenoviruses and group B coxsackieviruses. Proc Natl Acad Sci USA 94: 3352–3356.

Wickham TJ, Mathias P, Cheresh DA et al. (1993) Integrins αvβ3 and αvβ5 promote adenovirus internalization but not virus attachment. Cell 73: 309–319.

Wickham TJ, Filardo EJ, Cheresh DA et al. (1994) Integrin αvβ5 selectively promotes adenovirus mediated cell membrane permeabilization. J Cell Biol 127: 257–264.

Design of a pH-Sensitive Polymeric Carrier for Drug Release and Its Application in Cancer Therapy

Haruhiko Kamada, Yasuo Tsutsumi, Yasuo Yoshioka, Yoko Yamamoto, Hiroshi Kodaira, Shin-ichi Tsunoda, Takayuki Okamoto, Yohei Mukai, Hiroko Shibata, Shinsaku Nakagawa, and Tadanori Mayumi

Department of Biopharmaceutics, Graduate School of Pharmaceutical Sciences, Osaka University, Osaka, Japan

ABSTRACT

Purpose: **In this study, to optimize the polymeric drug delivery system for cancer chemotherapy, we developed a new pH-sensitive polymeric carrier, poly(vinylpyrrolidone-co-dimethylmaleic anhydride) [PVD], that could gradually release native form of drugs with full activity, from the conjugates in response to changes in pH. We examined the usefulness of PVD as a polymeric drug carrier.**

Experimental Design: **PVD was radically synthesized with vinylpyrrolidone and 2,3-dimethylmaleic anhydride, which is known to be a pH-reversible amino-protecting reagent. Conjugates between PVD and other drugs, such as Adriamycin (ADR), were prepared under the slightly basic conditions (pH 8.5). The drug-release pattern and the antitumor activity of PVD were examined.**

Results: **At pH 8.5, the release of the drugs from the conjugate was not observed. In contrast, PVD could release fully active drugs in the native form in response to the change in pH near neutrality, and gradually released drugs at neutral pH (7.0) and slightly acidic pH (6.0). The drug-release pattern in serum was almost similar to that observed during these physiological conditions. The PVD-conjugated ADR showed superior antitumor activity against sarcoma-180 solid tumor in mice, and it had less toxic side effects than free ADR. This enhancement in the antitumor therapeutic window may be due to not only the improvement of plasma half-lives and tumor accumulation of ADR, but also its controlled and sustained release from the conjugates *in vivo*.**

Conclusions: **These results indicate that PVD is an effective polymeric carrier for optimizing cancer therapy.**

INTRODUCTION

The major limitation of antitumor agents, typified by Adriamycin (ADR, doxorubicin), used in clinical applications, is its severe toxicity, such as bone marrow suppression and cardiotoxicity (1–4). This is caused by the high and frequent dose of antitumor agents, which have a very short half-life and a wide tissue distribution. The chemical conjugation of antitumor agents with water-soluble polymeric carriers has been found recently to overcome these drawbacks. The conjugation of low molecular weight antitumor agents to water-soluble polymeric carriers, such as *N*-(2-hydroxypropyl)methylacrylamide, divinylether-co-maleic anhydride, styrene-co-maleic anhydride, dextran, and polyethylene glycol (PEG), offers a potential mechanism to improve cancer chemotherapy (5–10). Distribution of the conjugates, which have a higher molecular weight, is usually restricted to the intravascular space after *i.v.* injection due to the low permeability in most organs with a continuous capillary bed. In contrast, these macromolecular conjugates preferentially accumulate in solid tumors due to the enhanced permeability and retention effect (11, 12). As a result, the polymeric drug delivery system (DDS) may selectively expand the therapeutic windows of antitumor agents.

However, there is a restriction on the clinical application of this polymeric DDS for cancer chemotherapy. For instance, after the ADR that is taken up into the tumor cells intercalates between double strands of DNA, its antitumor activity is induced by inhibition of DNA replication and topoisomerase activity in the tumor cells (13). However, the intercalation of polymer-conjugated ADR between double strands of DNA is based on macromolecular interactions, which are sterically hindered by the attached polymeric carrier. The introduction of polymeric carriers to antitumor agents, including ADR, is generally targeted at ionic functional groups in the antitumor agent, some of which may play an important role for their cytotoxic activity. Additionally, the conjugates with larger molecular size are hardly taken up into tumor cells through various transporters, because these transporters carry low molecular weight antitumor agents. Thus, for obtaining *in vivo* antitumor effects, a sufficient amount of antitumor agents is required to be released from the conjugates, because polymer-conjugated anticancer drugs themselves seldom show antitumor activity. However, in most cases, the conjugate between an antitumor agent and a polymeric carrier is formed through stable covalent bonding. As a result, the antitumor therapeutic effects of these conjugates have often not been observed in their clinical trials. To overcome these problems, a relatively unstable linker was used for the conjugation between an antitumor agent and a polymeric

Received 11/7/03; revised 12/25/03; accepted 12/31/03.
Grant support: Grant-in-Aid for Scientific Research (No. 15680014) from the Ministry of Education, Science and Culture of Japan, Health Sciences Research Grants for Research on Health Sciences focusing on Drug Innovation from the Japan Health Sciences Foundation (KH63124), and Takeda Science Foundation.
The costs of publication of this article were defrayed in part by the payment of page charges. This article must therefore be hereby marked *advertisement* in accordance with 18 U.S.C. Section 1734 solely to indicate this fact.
Note: H. Kamada, Y. Tsutsumi, and Y. Yoshioka contributed equally to the work.
Requests for reprints: Yasuo Tsutsumi, Department of Biopharmaceutics, Graduate School of Pharmaceutical Sciences, Osaka University, 1-6 Yamadaoka, Suita, Osaka 565-0871, Japan. Phone: 81-0-6-6879-8178; Fax: 81-0-6-6879-8178; E-mail: tsutsumi@phs.osaka-u.ac.jp.

carrier. Most of the antitumor agents released from the conjugates have a linker fragment. Furthermore, these modified antitumor agents show much lower specific activities than original antitumor agents in their native form, because the linker fragment is attached to an active functional group of the antitumor agents (14, 15). Thus, it is necessary to develop a novel polymeric DDS for optimization of cancer chemotherapy.

Dimethylmaleic anhydride (DMMAn) with a double bond in its structure is used as a pH-reversible protective reagent of amino groups in proteins and chemical compounds (16, 17). DMMAn binds to an amino group by forming an amide bond through its acid anhydride group over pH 8, and then reversibly dissociates from the amino group for change in pH to near slightly acidic from neutral. Thus, if a polymeric carrier with this function of DMMAn is synthesized, it will release a native drug in response to changes in pH. It is known that pH of both tumor and inflammatory tissues are slightly acidic unlike normal tissues (18). Thus, the conjugates between an antitumor agent and the polymeric modifier with the function of DMMAn may show superior plasma half-life and tumor accumulation compared with unconjugated antitumor agents and, therefore, effectively release the antitumor agents in native form in the tumor tissues.

In this study, to optimize the polymeric DDS for cancer chemotherapy, poly(vinylpyrrolidone-co-dimethylmaleic anhydride) [PVD] was radically synthesized with vinylpyrrolidone and DMMAn. ADR was used as a model antitumor agent and conjugated with PVD along with other drugs. Fully active drugs were gradually released from the conjugates in response to the change in pH. The PVD-conjugated ADR showed superior antitumor activity against S-180 sarcomas in mice and had less side effects than free ADR. These results indicate that PVD is an effective polymeric carrier for cancer therapy.

MATERIALS AND METHODS

Materials. DMMAn was purchased from AKROS (Aichi, Japan). Other reagents and solvents were obtained from standard sources.

Synthesis of PVD. PVD was synthesized by the radical polymerization method using 4,4'-azobis-4-cyanovaleric acid as a radical initiator. Briefly, DMMAn and vinylpyrrolidone were mixed in a ratio of 1:20 in a glass tube containing dimethyl formamide and incubated at 60°C for 6 h. The resulting copolymer was precipitated in dry diethyl ether, collected immediately after filtration, and dried under vacuum three times. The molecular weight was determined by gel-filtration chromatography (GFC; TSKgel G4000PW, TSKgel α-3000 columns; Tosoh, Tokyo, Japan). Polyvinylpyrrolidone (PVP) was also similarly synthesized. These polymers were separated into several fractions by GFC to obtain polymers with a narrow molecular weight distribution.

Conjugation of Lucifer Yellow Cadaverine (LYC) with PVD. An amino group of water-soluble fluorophore LYC (1.27 mg/300 μl of borate buffer; pH 8.5) was conjugated with PVD (6 mg) by forming an amide bond through its acid anhydride group. After the conjugation reaction for 30 min, the unconjugated free LYC was removed using 10-PG columns (Bio-Rad, Hercules, CA). PVD-modified LYC (PVD-LYC) was separated and purified by GFC. The release of free LYC from the PVD-LYC was not observed at pH 8.5. The solution of PVD-LYC was prepared to desired pH values and incubated at 37°C. Samples collected after various incubation times, went through desalting columns, and were analyzed for ratios between conjugated LYC and free LYC by measuring fluorescence intensity at 530 nm (emission) with excitation at 424 nm. The release of LYC from the conjugate in the serum was also measured by the same method after mixing it with an equal volume of mouse serum.

Toxicity of PVD. Monkey renal tubular (LLC-MK2) cells were seeded in 96-well plates at a concentration of 1.2×10^4 cells/well. After incubation for 24 h at 37°C, LLC-MK2 cells were incubated with PVD, PVP, PEG, and Polybrene at different concentrations. The plates were incubated for 24 h at 37°C, and cell viability was evaluated by 3-(4,5-dimethylthiazol-2-yl)-2,5-diphenyltetrazolium bromide (Dojindo, Kumamoto, Japan) assay as described by Mosmann (19) with minor modifications. Briefly, 3-(4,5-dimethylthiazol-2-yl)-2,5-diphenyltetrazolium bromide solution (5 mg/ml; 10 μl) was added into each well, and the cells were incubated at 37°C for 4 h. The resulting formazan product was dissolved by the addition of 100 μl of 10% SDS (Wako Pure Chemical Ind. Co., Ltd., Osaka, Japan) and 15 mM HCl. The solution was read on a microplate reader at 595 nm test wavelength with a reference wavelength of 655 nm.

Pharmacokinetic Analysis. PVD and PVP were dissolved in dimethyl formamide and activated for 24 h at room temperature with dicyclohexyl carbodiimide and *N*-hydroxysuccinimide, respectively. The polymers were incubated with thyramine hydrochloride for 24 h at 4°C, dialyzed in water, and lyophilized. Polymer-thyramine conjugates were radiolabeled by the chloramine-T method. ^{125}I-labeled polymer was purified by GFC. The clearance profiles of PVD and PVP (10 μg/mouse; 1×10^6 cpm/200 μl in saline) were studied after i.v. injection into the tail veins of ddY mice. Blood was collected from the tail vein at intervals, and radioactivity was measured. GFC analysis confirmed that >95% of the radioactivity in circulating blood 3 h after i.v. injection was derived from intact ^{125}I-PVD and ^{125}I-PVP. Mice were housed in metabolic cages to collect urine and sacrificed 3 h after treatment to evaluate tissue distribution.

Conjugation of ADR with PVD. PVD was dissolved in *N*-methyl-2-pyrrolidone at a concentration of 80 mg/4 ml. Then ADR (20 mg) was added to this solution. After the addition of triethylaminde (30 ml), the mixture was additionally incubated overnight at room temperature. After the reaction, distilled water was added, and pH of the mixture was adjusted to 8.5 by the addition of 0.2 M NaH_2PO_4. Unconjugated ADR was removed by ultrafiltration using a PM-30 (Amicon). The PVD-modified ADR (PVD-ADR) was then purified by dialysis. The amount of conjugated ADR was estimated by measuring its absorbance at 340 nm.

***In Vivo* Antitumor Activity of PVD-ADR.** *In vivo* antitumor effects of PVD-ADR were assessed by using ddY mice bearing mouse sarcoma-180 solid tumors. PVD-ADR and free ADR were injected i.v. to the mice at different doses, 60, 200, and 600 μg/mouse (ADR-equivalent dose) on days 7, 9, and 11 after tumor inoculation. The tumor volume was measured by a standard method as described elsewhere (20, 21).

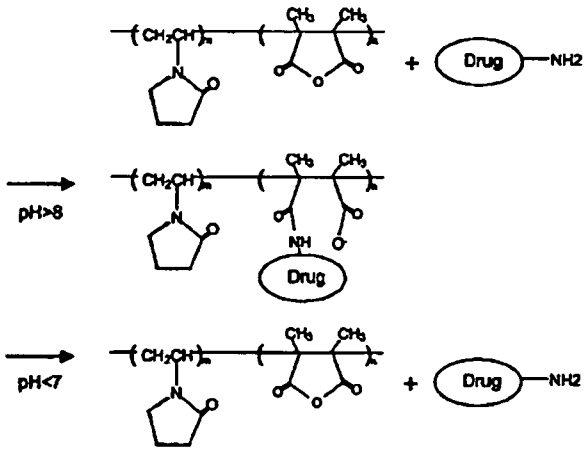

Fig. 1 Chemical structures and characteristics of poly(vinylpyrrolidone-co-dimethylmaleic anhydride).

RESULTS

Chemical Structure of PVD. For the radical synthesis of PVD, DMMAn was introduced at a ratio of 5% to the amount of vinylpyrrolidone. The average molecular weight of PVD was M_r 6,000 [Polydispersity (molecular weight/the number average molecular weight) = 1.14]. PVD was synthesized by radical copolymerization. Reflecting the properties of DMMAn, drugs were conjugated with PVD by forming an amide bond through its acid anhydride group of DMMAn to amino groups of drugs at more than pH 8.0 and released at lower than pH 7.0 (Fig. 1).

The pH-Sensitive Drug (LYC) Release from PVD-Conjugated LYC. The release of LYC as a model drug, which is a fluorophore with an amino group, from PVD-LYC was assessed. The release of LYC from PVD-LYC was time dependent, and the release speed increased with an increase in the pH (Fig. 2). At pH 8.5, a weak basic condition, almost no release or <1% release of LYC was observed. However, ~6% of the total LYC was released at pH 6.0 after 24 h incubation. Additionally, ~3% of the LYC was gradually released at pH 7.0 after 24 h of incubation. When PVD-LYC was incubated in the serum, results similar to the LYC release pattern at pH 6.0 were obtained.

Cytotoxicity of PVD. The *in vitro* cytotoxicity of PVD was assessed for clarifying its usefulness as a polymeric drug carrier. PVP and PEG had no effect on LLC-MK2 cells, whereas the cationic polymer, Polybrene, which is known to be an antitumorigenic agent, showed considerable cytotoxicity (Fig. 3). In contrast, PVD was not cytotoxic at concentrations up to 3 mg/ml. Evidently, PVD as well as PVP and PEG had no cytotoxic effect on human endothelial cells (data not shown).

Pharmacokinetics of PVD after i.v. Administration. The pharmacokinetics of PVD and PVP after i.v. administration were studied for 3 h (Fig. 4). PVP was separated and purified by GFC to adjust the molecular weight and polydispersity of PVD. PVD was effectively retained in blood as compared with PVP, although PVP was found previously to have the longest plasma half-life and to be the most suitable polymeric drug carrier for localizing the conjugated drug in blood. The half-lives of PVD and PVP were ~10 min and 30 min, respectively.

***In Vivo* Antitumor Effect of PVD-ADR.** To clarify the usefulness of PVD as a polymeric drug carrier for optimization of cancer chemotherapy, we synthesized PVD-ADR and compared its antitumor potency with that of ADR alone (Fig. 5 and 6, Table 1). Through GFC analysis, we confirmed that PVD-ADR was composed of one PVD molecule and one ADR molecule. As shown in Fig. 6, all of the mice administered with free ADR at a dose of 600 μg/mouse and 200 μg/mouse died

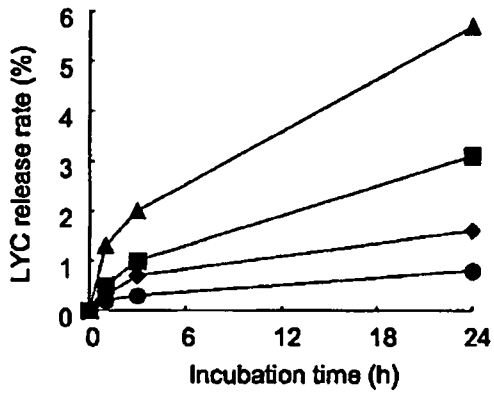

Fig. 2 pH-sensitive controlled release of lucifer yellow cadaverine (*LYC*) from the conjugates between poly(vinylpyrrolidone-co-dimethylmaleic anhydride) [PVD] and LYC. The release of LYC from the PVD-conjugated LYC (PVD-LYC) was assessed at indicated time intervals. Small molecule fractions collected after desalting gel-filtration chromatography were assigned as free LYC released from the macromolecular conjugates of PVD-LYC. The concentration of free LYC was measured by fluorescence intensity at 530 nm (excitation, 424 nm). The amounts of free LYC, relative to that of initiate PVD-conjugated LYC, are shown on the vertical axis. ▲, pH 6.0; ■, pH 7.0; ●, pH 8.5; ◆: serum.

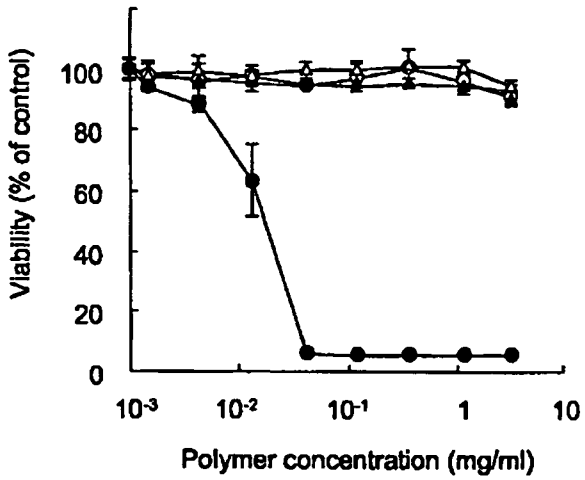

Fig. 3 Cytotoxicity of various polymeric carriers against LLC-MK2 cells. LLC-MK2 cells were incubated with various polymeric carriers for 24 h. Viability of the cells was determined by 3-(4,5-dimethylthiazol-2-yl)-2,5-diphenyltetrazolium bromide assay. Each value is mean (n = 3); *bars*, ± SD. ▲, polyethylene glycol; △, polyvinylpyrrolidone; ●, Polybrene; ○, poly(vinylpyrrolidone-co-dimethylmaleic anhydride).

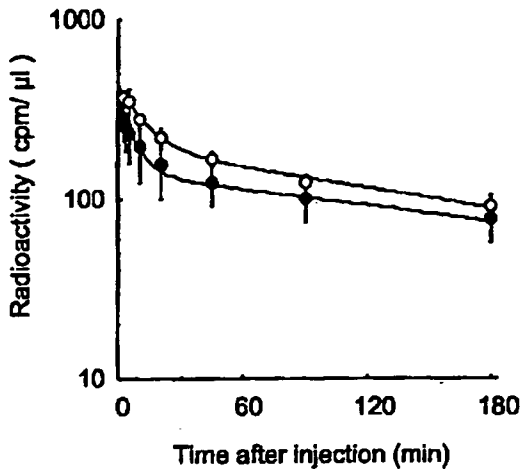

Fig. 4 Blood residency of polyvinylpyrrolidone (PVP) and poly(vinylpyrrolidone-co-dimethylmaleic anhydride) [PVD] after their i.v. administration. ^{125}I-labeled PVP and ^{125}I-labeled PVD were i.v. administered to normal ddY mice, and the radioactivity in blood was measured. The *curved line* was drawn by using the least-squares method based on measured values at indicated time intervals. Mice were used in groups of 4. Each value is mean; *bars*, ± SE. O, PVP; ●, PVD.

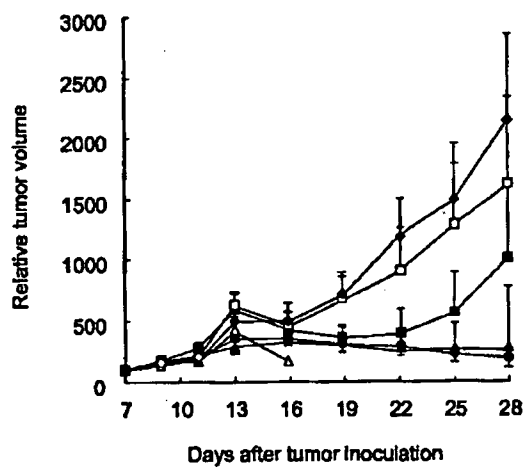

Fig. 5 Antitumor effects of Adriamycin (ADR) and poly(vinylpyrrolidone-co-dimethylmaleic anhydride) [PVD]-ADR on sarcoma-180 solid tumors. The ADR and PVD-ADR were i.v. administered to sarcoma-180 solid tumor-bearing mice on days 7, 9, and 11, after tumor inoculation. Data were expressed as relative tumor volume by the following equation: Relative tumor volume = mean tumor volume at a given time/mean tumor volume on day 7. Mice were used in groups of 4. Each value is mean; *bars*, ± SE. Intact mice, ◆. *Open symbol*, free ADR-treated mice. O, 600 μg/mouse/day; △, 200 μg/mouse/day; □, 60 μg/mouse/day. *Closed symbol*, PVD-ADR-treated mice. ●, 600 μg/mouse/day; ▲, 200 μg/mouse/day; ■, 60 μg/mouse/day.

within 6–10 days after their i.v. administration (within 13 days or 17 days after tumor inoculation) because of toxicity of ADR. There was a marked weight loss in these mice after the high dose of free ADR (data not shown). In mice treated with free ADR at a dose of 60 μg/mouse, although tumor growth was slightly inhibited without causing sudden death or weight loss (Figs. 5 and 6), complete tumor regression, defined as disappearance of tumor without regrowth within 100 days, was not observed (Table 1). Similar results were also observed in mice administered with a mixture of PVD and free ADR due to side effects (data not shown). In contrast, the antitumor activity of PVD-ADR at a dose of 60 μg ADR/mouse was more effective than that of free ADR at 60 μg/mouse (Fig. 5). Tumor growth was remarkably and completely inhibited by PVD-ADR at a dose of 200 μg ADR/mouse and 600 μg ADR/mouse (Fig. 5). Complete tumor regression was observed in 75%, 25%, and 25% of mice treated with PVD-ADR at a dose of 600 μg ADR/mouse, 200 μg ADR/mouse, and 60 μg ADR/mouse, respectively (Table 1). During the experimental period, all doses of PVD-ADR were well tolerated, and no loss in body weight was observed (Fig. 6).

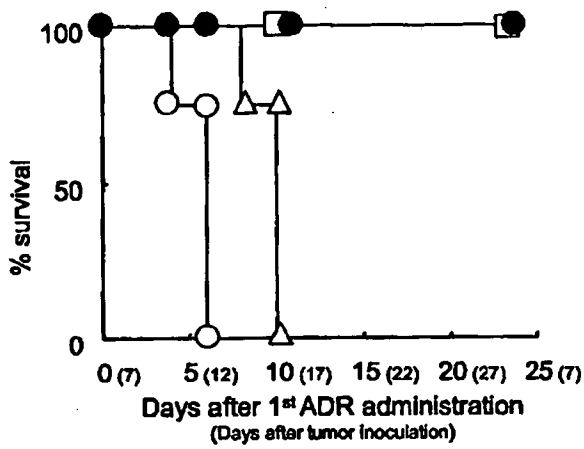

Fig. 6 Survival time of the sarcoma-180 tumor-bearing mice treated with Adriamycin (ADR) and poly(vinylpyrrolidone-co-dimethylmaleic anhydride) [PVD]-ADR. The ADR and PVD-ADR were i.v. administered to sarcoma-180 solid tumor-bearing mice on days 7, 9, and 11, after tumor inoculation. Mice were used in groups of 4. Survival time of treated-mice after i.v. administration of ADR and PVD-ADR were shown as the survival rate (%). *Open symbol*, free ADR. O, 600 μg/mouse/day; △, 200 μg/mouse/day; □, 60 μg/mouse/day. *Closed symbol*, PVD-ADR. ●, 600 μg/mouse/day; ▲, 200 μg/mouse/day; ■, 60 μg/mouse/day.

Table 1 Antitumor effects of ADR[a] and PVD-ADR on sarcoma-180 solid tumors

Complete regression was defined when tumor was not regrown for >100 days.

	Dose (μg/mouse/day)	Complete regression
ADR	600	All mice died in 13 days
	200	All mice died in 17 days
	60	0/4
PVD-ADR	600	3/4
	200	1/4
	60	1/4

[a] ADR, Adriamycin; PVD, poly(vinylpyrrolidone-co-dimethylmaleic anhydride).

DISCUSSION

In this study, to optimize the polymeric DDS for cancer chemotherapy, we attempted to develop a novel polymeric carrier that could release a native form of drugs in response to changes in pH near the neutrality. As described in the "Introduction," there are certain characteristics needed by the polymeric drug carrier: (*a*) to be excellent in blood residency for effectively obtaining the enhanced permeability and retention effect in tumors; (*b*) to gradually release the fully active form (native form) of antitumor agents; and (*c*) to efficiently release the native antitumor agents under the slightly acidic conditions, if possible, because it is known that the pH of tumor tissues is slightly lower than that of normal tissues (18). From such a viewpoint, some polymeric carriers, typified by divinylether-co-maleic anhydride and styrene-co-maleic anhydride, were developed (6, 7). Some maleic anhydride, that is one of the acid anhydride, were contained in the structure of these polymeric carriers, and the antitumor agents were conjugated with these polymeric carriers via the formation of amide bonds between the amino group of antitumor agents and the acid anhydride groups. However, the amide bonds formed through maleic anhydride are very stable near neutral pH, and the antitumor agents are released from the conjugates under strong acidic conditions (<pH 3). As a result, the antitumor therapeutic effects of these conjugates have often not been observed in their clinical trials. In contrast, DMMAn binds to an amino group by forming an amide bond through its acid anhydride group over pH 8, and then reversibly dissociates from the amino group on change in pH to slightly acidic from neutral. However, there are no reports about DMMAn-introduced carrier.

For enhancing the blood residency of drugs, PVP was found to be one of the most useful polymeric carriers, because the plasma half-life of PVP itself was much longer than those of PEG and other polymeric modifiers (21, 22). In fact, PVP-conjugated tumor necrosis factor (TNF)-α showed a higher half-life than PEG-conjugated TNF-α despite having the same molecular size (21). As a result, PVP-conjugated TNF-α had a more potent antitumor effect than PEG-conjugated TNF-α, without any toxic side effects. This phenomenon has also been observed in PVP-conjugated interleukin 6 and leukemia inhibitory factor (22). Furthermore, PVP can be introduced in various useful functional groups by radical copolymerization (23). Additionally, the safety of PVP has been clinically confirmed. Using PVP as a backbone polymer, we synthesized PVD as a novel polymeric carrier for the development of antitumor polymeric DDS. Reflecting the property of DMMAn, the conjugate between PVD and drugs (LYC) could gradually release the native drugs directly (nonlinker) by responding to a change in pH near neutrality (Fig. 2). As shown in Fig. 3, the safety of PVD appears to be similar to PEG and PVP, which are used clinically. Additionally, the plasma half-life of PVD was longer than that of parental PVP (Fig. 4). These results strongly suggested that PVD may be useful as a polymeric drug carrier for cancer chemotherapy.

We show here that the conjugation of ADR with PVD increases its antitumor activity while decreasing its nonspecific toxicity (Figs. 5 and 6; Table 1). Overall, the therapeutic window is markedly increased. These results have important clinical implications for the use of antitumor chemotherapeutic agents in patients. The expansion of the therapeutic window is probably due to the following reasons. It is known that vascular permeability of macromolecules into solid tumors and its retention in tumor tissues are enhanced compared with normal tissues. This is generally called the enhanced permeability and retention effect (11, 12). Thus, this enhanced permeability and retention effect may effectively accumulate the PVD-ADR in tumors. Additionally, as it is known that pH of tumor tissues is slightly lower than that of normal tissues, the PVD-ADR is likely to release free ADR more efficiently in tumor tissues (18). But detailed studies on the pharmacokinetics of PVD-ADR are necessary to clarify the mechanism of its wider therapeutic window, and these are currently under investigation.

To improve the therapeutic bioavailability of bioactive proteins, bioactive proteins have been conjugated with water-soluble polymers such as PEG (24). PEGylation of proteins increases their molecular size and enhances steric hindrance, both of which are dependent on PEG attached to the protein. This results in the improvement of the plasma half-lives of proteins and stability against proteolytic cleavage as well as a decrease in its immunogenicity. We also reported that PEGylation of proteins, such as TNF-α, interleukin 6, and immunotoxin, could enhance therapeutic potency and could reduce undesirable side effects (21–23, 25–27). However, there is a restriction to this approach, because PEGylation is frequently accompanied with a significant loss of specific activity of a protein. Lysine amino groups of proteins are often used for PEGylation because they are highly reactive. This PEGylation, however, is nonspecific and occurs at the NH_2 terminus as well as at all of the internal lysine residues in proteins, some of which may be in or near their active site. Resultant PEGylated proteins are heterogeneous and show significantly lower bioactivity. These problems remarkably limit the clinical application of PEGylated proteins. The present study shows that PVD effectively releases fully active drugs in the native form at neutral pH ranges and is a safe drug carrier that has no cytotoxicity. Additionally, PVD may be a suitable polymeric carrier for the prolongation of plasma half-life of drugs as well as PVP, rather than PEG. Thus, we are now attempting to design the PVD-conjugated cytokines for promotion of protein therapies against solid and metastatic tumors.

In conclusion, we developed a new polymeric carrier, PVD, that could gradually release native drugs from the conjugate in response to changes in pH near neutrality. The PVD-ADR showed superior antitumor activity and had less side effects than free ADR. This enhancement of the antitumor therapeutic window may be due to not only the improvement of plasma half-lives and tumor accumulation of ADR, but also its controlled and sustained release from the conjugates *in vivo*. These results indicate that PVD is an effective polymeric carrier for cancer therapy.

REFERENCES

1. Praga C, Beretta G, Labianca R. Cardiac toxicity from antitumor therapy. Oncology (Basel) 1980;37:51–8.

2. Wadler S, Fuks JZ, Wiernik PH. Phase I and II agents in cancer therapy: I. anthracyclines and related compounds. J Clin Pharmacol 1986:26:491–509.

3. Bristow MR, Billingham ME, Mason JW, Daniels JR. Clinical spectrum of anthracycline antibiotic cardiotoxicity. Cancer Treat Rep 1978; 62:873–9.

4. Sparano JA. Doxorubicin/taxane combinations: cardiac toxicity and pharmacokinetics. Semin Oncol, 1999;26:14–9.

5. Seymour LW, Ulbrich K, Steyger PS, et al. Tumour tropism and anti-cancer efficacy of polymer-based doxorubicin prodrugs in the treatment of subcutaneous murine B16F10 melanoma. Br J Cancer 1994;70: 636–41.

6. Yamamoto H, Miki T, Oda T, et al. Reduced bone marrow toxicity of neocarzinostatin by conjugation with divinyl ether-maleic acid copolymer. Eur J Cancer 1990;26:253–60.

7. Maeda H. SMANCS and polymer-conjugated macromolecular drugs: advantages in cancer chemotherapy. Adv Drug Deliv Rev 2001;46:169–85.

8. Senter PD, Svensson HP, Schreiber GJ, Rodriguez JL, Vrudhula VM. Poly(ethylene glycol)-doxorubicin conjugates containing β-lactamase-sensitive linkers. Bioconjug Chem 1995;6:389–94.

9. Matsumoto S, Yamamoto A, Takakura Y, Hashida M, Tanigawa N, Sezaki H. Cellular interaction and in vitro antitumor activity of mitomycin C-dextran conjugate. Cancer Res 1986;46:4463–8.

10. Kabanov AV, Okano T. Challenges in polymer therapeutics: state of the art and prospects of polymer drugs. Adv Exp Med Biol 2003; 519:1–27.

11. Maeda H, Sawa T, Konno T. Mechanism of tumor-targeted delivery of macromolecular drugs, including the EPR effect in solid tumor and clinical overview of the prototype polymeric drug SMANCS. J Control Release 2001;74:47–61.

12. Kopecek J, Kopeckova P, Minko T, Lu ZR, Peterson CM. Water soluble polymers in tumor targeted delivery. J Control Release 2001; 74:147–58.

13. Denny WA. DNA-intercalating ligands as anti-cancer drugs: prospects for future design. Anticancer Drug Des 1989;4:241–63.

14. Duncan R, Spreafico F. Polymer conjugates. Pharmacokinetic considerations for design and development. Clin Pharmacokinet 1994;27: 290–306.

15. Duncan R, Seymour LW, O'Hare KB, et al. Preclinical evaluation of polymer-bound doxorubicin. J Control Release 1992;19:331–46.

16. Butler PJ, Harris JI, Hartley BS, Leberman R. Reversible blocking of peptide amino groups by maleic anhydride. Biochem J 1967;103:78–9.

17. Butler PJ, Harris JI, Hartley BS, Lebeman R. The use of maleic anhydride for the reversible blocking of amino groups in polypeptide chains. Biochem J 1969;112:679–89.

18. Wike-Hooley JL, Haveman J, Reinhold HS. The relevance of tumour pH to the treatment of malignant disease. Radiother Oncol 1984; 2:343–66.

19. Mosmann T. Rapid colorimetric assay for cellular growth and survival: application to proliferation and cytotoxicity assays. J Immunol Methods 1983;65:55–63.

20. Haranaka K, Satomi N, Sakurai A. Antitumor activity of murine tumor necrosis factor (TNF) against transplanted murine tumors and heterotransplanted human tumors in nude mice. Int J Cancer 1984;34: 263–7.

21. Kamada H, Tsutsumi Y, Yamamoto Y, et al. Antitumor activity of tumor necrosis factor-α conjugated with polyvinylpyrrolidone on solid tumors in mice. Cancer Res 2000;60:6416–20.

22. Tsunoda S, Kamada H, Yamamoto Y, et al. Molecular design of polyvinylpyrrolidone-conjugated interleukin-6 for enhancement of in vivo thrombopoietic activity in mice. J Control Release 2000;68:335–41.

23. Kamada H, Tsutsumi Y, Sato-Kamada K, et al. Synthesis of a poly(vinylpyrrolidone-co-dimethyl maleic anhydride) co-polymer and its application for renal drug targeting. Nat Biotechnol 2003;21:399–404.

24. Youngster S, Wang YS, Grace M, Bausch J, Bordens R, Wyss DF. Structure, biology, and therapeutic implications of pegylated interferon α-2b. Curr Pharm Des 2002;8:2139–57.

25. Tsunoda S, Ishikawa T, Watanabe M, et al. Selective enhancement of thrombopoietic activity of PEGylated interleukin 6 by a simple procedure using a reversible amino-protective reagent. Br J Haematol 2001;112:181–8.

26. Tsutsumi Y, Onda M, Nagata S, Lee B, Kreitman RJ, Pastan I. Site-specific chemical modification with polyethylene glycol of recombinant immunotoxin anti-Tac(Fv)-PE38 (LMB-2) improves antitumor activity and reduces animal toxicity and immunogenicity. Proc Natl Acad Sci USA 2000;97:8548–53.

27. Yamamoto Y, Tsutsumi Y, Yoshioka Y, et al. Site-specific PEGylation of a lysine-deficient TNF-α with full bioactivity. Nat Biotechnol 2003;21:546–52.

YAKUGAKU ZASSHI 124(11) 769—780 (2004) © 2004 The Pharmaceutical Society of Japan

—Reviews—

プロテオーム創薬に叶うDDS基盤技術の開発

堤　康央[1)]

Development of Novel DDS Technologies for Pharmacoproteomic-based Drug Discovery and Development

Yasuo TSUTSUMI[1)]

Department of Biopharmaceutics, Graduate School of Pharmaceutical Sciences, Osaka University, 1-6 Yamadaoka, Suita 565-0871, Japan

(Received July 1, 2004)

With the success of the Human Genome Project, the focus of life science research has shifted to the functional and structural analyses of proteins, such as proteomics and structural genomics. These novel approaches to the analysis of proteins, including newly identified ones, are expected to help in the identification and development of protein therapies for various diseases. Thus pharmacoproteomic-based drug discovery currently has a very high profile. Nevertheless, the use of bioactive proteins in the clinical setting is not straightforward because *in vivo* these proteins have low stability and pleiotropic action. To promote pharmacoproteomic-based drug discovery and development, we have attempted to establish a system for creating functional mutant proteins (muteins) with the desired properties and to develop a site-specific bioconjugation system for further improving their therapeutic potency. These innovative protein-drug systems are discussed in this review.

Key words——phage display system; proteomics; bioconjugation; protein therapy; targeting

1. はじめに

20世紀後半の遺伝子・蛋白質工学や分子細胞生物学の目覚ましい進歩も相まって，疾病治療に有望視された種々生理活性蛋白質が同定され，サイトカインを初めとする蛋白質が難治性疾患に対する“夢の治療薬”として期待された．この流れは昨今のヒトゲノムプロジェクトの完了宣言を受け，さらに加速度を増してきている．すなわちヒトゲノム解読により，約3万種の遺伝子のうち半数は未知蛋白質をコードしており，これらの中には疾病に深く関与する蛋白質，言い換えれば医薬品シーズや創薬ターゲットとなり得る疾患関連蛋白質が多数含まれるものと期待されている．その結果，創薬を指向したポストゲノム研究は，疾患状態における多種多様な蛋白質の時空間的・質量的な発現様式と疾患の発症・増悪・治癒との連関を網羅的に解析しようとする疾患プロテオミクスなどへと集約されつつある．そのため，疾患プロテオミクス情報などを有効活用し，疾病治療に有効な蛋白質を創製しようとするプロテオーム創薬に大きな注目が集まっている．

周知の通り，20世紀後半には数多くの生理活性蛋白質が同定され，種々難治性疾患に対して臨床応用が試みられた．しかしながら，これら生理活性蛋白質は切れ味鋭い作用を有するものの，その生体内安定性が極めて乏しいために，臨床応用する際には生体内のホメオスタシスを無視した大量頻回投与を余儀なくされ，重篤な副作用を招いてしまう．さらには，サイトカインなどは一般に複数種のレセプターを介し，多様な *in vivo* 生理活性を有するために，目的とする治療作用以外の作用をも同時に発現してしまう．そのため，生理活性蛋白質の臨床応用は著しく制限されており，そのほとんどが医薬品化されていない．したがって，疾患プロテオミクス情報などを有効活用したプロテオーム創薬を推進し，有効かつ安全な蛋白療法を確立していくためには，これら蛋白質固有の問題点を克服し得る創薬テクノロジー，すなわち蛋白療法の最適化を目指した

大阪大学薬学研究科薬剤学分野（〒565-0871 吹田市山田丘1-6）
e-mail: ytsutsumi@nihs.go.jp
本総説は，平成16年度日本薬学会奨励賞の受賞を記念して記述したものである．

DDS (Drug Delivery System) の確立が依然として必須となっている．この創薬テクノロジーは，言わば疾患プロテオミクス研究といったポストゲノム基礎研究とプロテオーム創薬や蛋白療法との架け橋になるものと考えられる．

本観点から現在，1) レセプター親和性・特異性などが高く医薬価値に優れた機能性人工蛋白質を迅速創製できる蛋白質分子進化戦略の構築，[2] 2) 蛋白質の生体内安定性を向上させ，かつ目的治療作用の選択的発現能を付与できる高分子バイオコンジュゲーション法の確立，[2,3] 3) DDS 機能（標的指向能・薬物徐放化能等）を有した機能化高分子キャリアの設計[4]に焦点を絞り，上記3者を融合させた「プロテオーム創薬に叶う DDS 基盤テクノロジー」の確立を図っている．本稿では，紙面の許す限り詳細に，上述した 1)—3) の DDS 基盤テクノロジーについて紹介させて頂く．

2. 医薬価値に優れた機能性人工蛋白質の創製システムの構築

蛋白療法の最適化に向け，従来から産・官・学の多くのバイオ研究機関が，特定レセプターへの親和性や選択性に優れた“生理活性蛋白質のアミノ酸置換体（機能性人工蛋白質）”を創製するため，Kunkel 法などの点突然変異法を用いた構造変異体の作製を精力的に試みている．[3,5] しかし点突然変異法では，まず構造変異体の立体構造や機能をシミュレーションし，トライ・アンド・エラーで生理活性蛋白質の構成アミノ酸を1つずつ別の特定アミノ酸に改変することにより，個々の構造変異体を作製せねばならない．そのうえで目的とする機能性人工蛋白質を同定するため，作製した構造変異体の機能を個別に評価する必要がある．そのため従来法では，膨大な時間・労力を費やすばかりか，作製し得る構造変異体の多様性（種類）にも限界があり，期待通りの成果は得られていないのが現状である．

一方で近年，バクテリオファージの生活環を巧みに利用し，ターゲット（分子・粒子・細胞）への高親和性結合分子を網羅的かつ迅速に探索・同定し得る基盤技術としてファージ表面提示法が考案された[6] (Fig. 1)．このファージ表面提示法の際立った特徴は，1) g3p などのファージ外殻蛋白質をコードした遺伝子の 5′末端領域に，任意の外来性遺伝子を組み込んだファージゲノム（若しくはファージミドベクター）を構築することで，その外来性遺伝子産物をターゲットと相互作用可能な状態でファージ表面に提示できること，2) 個々のファージ粒子を観た場合，遺伝型（ファージ粒子に内封されている外来性遺伝子）と表現型（ファージ表面に提示された蛋白質）が一致していること（1個の宿主菌に1個のファージしか感染し得ないことに起因する），3) 別々の外来性遺伝子産物を表面提示したファージを数十億種類以上の多様性に富んだライブラリとして容易に調整できること，4) 宿主菌に感染させることで簡便に特定ファージやライブラリファージを増幅できることなどにある．そのため，ファージ表面に数千万から数十億種類以上もの多様性に富んだランダムペプチドやナイーブ抗体，cDNA 由来蛋白質などを発現させたファージライブラリを構築し，このライブラリの中から，ターゲットへ高親和性に結合するファージを選択・回収，増幅するという操作（パンニング）を繰り返すことにより，ターゲットに対する高親和性結合分子を表面提示したファージのみを濃縮・選択できる．しかも得られたファージは目的の蛋白質をコードする遺伝子を内封しているため，その遺伝子配列をも同時に得られる．そのため，このファージ表面提示法は様々な結合分子を迅速かつ網羅的にスクリーニングし得る基盤技術として，その応用範囲が急速に広がりつつある．しかしながらこのファージ表面提示法は，現在までのところ特定ターゲットに親和性を有する抗体やペプチドを同定する手段として利用されているに過ぎなかった．そもそもサイトカインなどの生理活性蛋白質をファージ表面に提示させた例すら皆無であった．

本研究では以上の点に着目し，ファージ表面提示法を独自に改良することにより 10^8 種類以上もの多様性を有した構造変異蛋白質（生理活性蛋白質のアミノ酸置換体）を一挙に Combinatorial Biosynthesis し，この構造変異体ライブラリの中から，レセプター親和性や特異性などが向上した“医薬価値に優れた機能性人工蛋白質”を迅速かつ効率良く同定できる「プロテオーム創薬のための蛋白質分子進化戦略」を確立した．[2] ここでは一例として腫瘍壊死因子（Tumor necrosis factor-α; TNF-α）をモデルとした機能性人工蛋白質の創製に関して述べさせていただく．

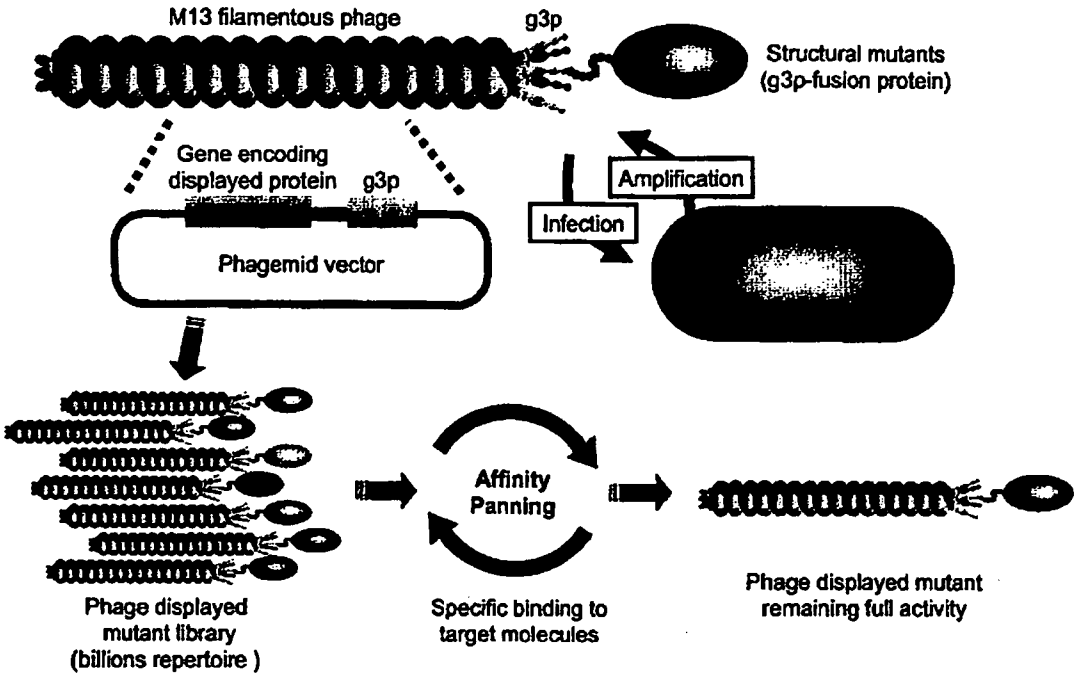

Fig. 1. Creation of Functional Mutein Using Phage Display System

Phage display system has the following main characteristics: 1) proteins can be displayed on the outer shell of the phage where they can interact with their target molecules, such as a receptor or antigen. These protein-displaying phage particles are produced by the integration of a foreign gene into the 5'-terminus of the gene that encodes the outer shell of the phage (*i.e.* g3p) in phagemid vector or phage genome; 2) the genotype of this phage (the foreign gene inside the phage clone), corresponds with the phenotype (the protein displayed on the phage's surface); 3) phage particles or "libraries", can readily be made, which consist of billions of varieties of protein; 4) a selected phage from the library can be readily amplified by infection of a host bacterial cell. It is therefore possible to screen for, and then isolate, high-affinity binders to target molecules from the phage library. Additionally, since isolated phage clones contain a gene sequence that codes for the desired protein, this also allows information of their amino acid sequence to be obtained.

3. 医薬価値に優れた機能性人工 TNF-α の創製

TNF-α は，BCG（Bacillus Calmette-Guerin）感作マウスにリポ多糖（LPS）を投与した際に血液中に検出され，さらに Meth-A 繊維芽肉腫の出血壊死を惹起する生理活性蛋白質として 1975 年に見出された.[7] TNF-α は 157 個のアミノ酸からなる分子量 17000，等電点 5.3 の生理活性蛋白質であり，その分子構造内に 6 個のリジン残基を含有している.[8] また，痕跡程度に糖鎖を有していることや分子内ジスルフィド結合を有していることが知られている．さらに TNF-α は，水溶液中では 2 枚の β シートが折り重なったサンドウィッチ状の構造を形成し，ホモフィリックな三量体として存在する.[9]

当初 TNF-α は，*in vitro* における検討から，腫瘍細胞に対しては細胞傷害性を示すものの，正常組織細胞に対してはほとんど傷害性を示さないものと考えられていた.[10,11] そのため，1980 年代に飛躍的進歩を遂げた遺伝子工学技術により大量生産可能となった TNF-α を「夢の抗癌剤」として，臨床応用しようとする試みがセンセーショナルに進められてきた.[12] しかしながら，ほかの生理活性蛋白質でも観られたように，TNF-α は体内安定性が極めて乏しいために（血中半減期；数分から数十分程度），臨床応用の際には，生体内のホメオスタシスを無視した大量頻回投与を余儀なくされ，発熱，悪心，嘔吐，血圧低下，消化管障害，エンドトキシン様ショックなど，非常に強い副作用を招いてしまった.[13—15] これら重篤な副作用のため，全身性の抗腫瘍薬として TNF-α を用いる場合，その投与量は抗腫瘍作用発現に必要な量のわずか 1/5—1/25 に制限せざるを得ないものと結論付けられた．そのため，現在の TNF-α による癌化学療法では，局所投与（腫瘍内投与や癌支配動脈への動脈内投与）に限定されてしまっている.[16—18] しかし一方で，この TNF-α の局所投与による固形癌の奏功率は目を見張るものがあり，依然として TNF-α の全身性抗癌剤としての適用のみならず，腫瘍血管における物質透過性の選択的亢進剤や抗腫瘍免疫活性化剤として

の全身的応用に期待が持たれている．以上の課題は，インターフェロン-γ，インターロイキン-2を始めとするサイトカインだけでなく，数多くの生理活性蛋白質にも当てはまることである．[19—21]

さて，TNF-αの抗腫瘍作用は，1）直接的な腫瘍細胞傷害，2）血中の抗腫瘍エフェクター免疫細胞の活性化，3）腫瘍血管の特異的崩壊により発現するものと考えられている（Fig. 2）．[22] なかでも3）の腫瘍出血壊死作用は，正常血管のみならず炎症部位新生血管でさえ全く生じず，TNF-αの特筆すべき特異性の高い抗腫瘍効果であることを認めている．[23] しかし，最近まではこの腫瘍血管に対する選択的な作用機構の詳細はあまり知られていなかった．これまでの研究から，血管内皮細胞は，周りの組織細胞から分泌される液性因子や細胞外マトリックスなどの影響により組織特有の性質を保持形成しており，この組織特異的な性質は，*in vitro* においてCo-cultureや培養上清（ならし培地）などを用いた系によって再現できることを見出している．[24,25] そこで，各種腫瘍細胞の培養上清を用いて血管内皮細胞を培養することにより，腫瘍環境下における血管内皮細胞のTNF-α感受性を検討した．通常の培養条件（10% FCSを含むDMEM培地）や正常な血管内皮細胞の培養上清を用いて培養した場合は，1000単位/mlのTNF-α濃度においても血管内皮細胞は全く傷害を受けず，高いTNF-α抵抗性が観察された．一方，Meth-A繊維芽肉腫細胞の培養上清で培養した血管内皮細胞では，わずか10単位/mlのTNF-α濃度で著明な障害性が認められた．この現象は，B16-BL6メラノーマ細胞やColon-26アデノカルシノーマ細胞などの他の腫瘍細胞の培養上清でも観察され，Meth-A繊維芽肉腫細胞の培養上清と同様にTNF-αに対する血管内皮細胞の感受性が上昇した．以上のことからTNF-αは，多くの腫瘍株に対して腫瘍血管を特異的に傷害することで，抗腫瘍効果を示すものと考えられた．加えて，最近の報告では腫瘍血管内皮細胞におけるEndothelial monocyte activating polypeptide II（EMAP II）の発現が，TNF-αの抗腫瘍作用の選択的発現に重要な役割を担っていることも示唆されている．[26] すなわち，TNF-αの血中滞留性を向上させることは，前述の1）から3）に示したTNF-αの抗腫瘍作用のすべてを活性化することにつながるものと考えられる．また，血中から肝臓などの血管外組織に移

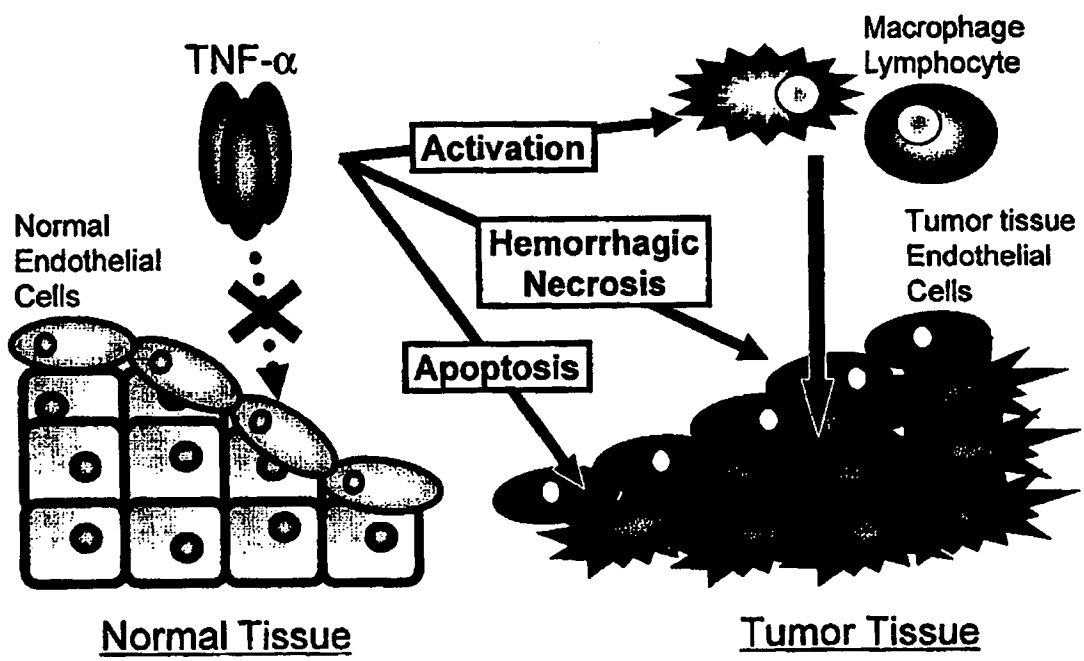

Fig. 2. Mechanism of Anti-Tumor Effect of TNF-α

The anti-tumor effect of TNF-α is known to result not only from its direct cytotoxicity against tumor cells but also from activation of anti-tumor effecter immune cells in the blood, such as macrophages, cytotoxic lymphocytes, and neutrophils, and furthermore from specific damage to tumor blood vessels.

行してしまったTNF-αが副作用の主因となるため,[27,28] 血中滞留性の向上に伴う正常組織への移行性の低下は，副作用軽減にも直結するものと期待できる.

以上の観点から，本研究ではTNF-αをモデル蛋白質と捉え，レセプター親和性や生物活性，血中滞留性などが向上したリジン欠損TNF-αを創製することで初めて可能となる，後述の"部位特異的高分子バイオコンジュゲーション法"を適用することで，TNF-αの血中滞留性・体内安定性をさらに向上させ，TNF-αの多様な *in vivo* 作用の中から目的とする抗腫瘍作用のみを選択発現させることを試みた.

さてTNF-αの場合，アラニン・スキャンといった従来の点突然変異法を用いた構造-活性相関研究により，TNF-αのLys11やLys65・Lys90はその立体構造（三量体）形成やレセプター結合に必須と言われていた．これはTNF-αに限らず，一般にリジン残基は多くの場合，生理活性蛋白質の高次構造形成やリガンド-レセプター結合などに必須の役割を担っているため，他のアミノ酸への置換は致命的な活性低下を招いてしまうことが，従来までの点突然変異解析によって常識となっていた．事実これまで，蛋白質中のリジン残基すべてを欠損させ得た例（リジン欠損体）は皆無であった．しかしわれわれはこの既成概念を覆す知見，すなわちLys11やLys65・Lys90を含む全6個のリジン残基を一挙に他のアミノ酸へ置換しても，wild型TNF-α（wTNF-α）と同等さらには10倍以上もの生物活性を有するリジン欠損TNF-αを創製することに初めて成功した（Fig. 3）．このwTNF-αと同等以上の生物活性を有する種々のリジン欠損TNF-αは，BIAcoreを用いたTNFレセプターIやTNFレセプターIIへの結合性評価により，wTNF-αと同等以上のレセプター親和性を有していること，超遠心解析やゲル濾過解析から三量体を形成していることも確認している．これらの知見は，TNF-α分子中の全6個のリジン残基を他のアミノ酸へ一挙かつ網羅的に置換した20^6（6400万）種類もの構造変異TNF-α（アミノ酸置換体）を表面提示したファージライブラリを作製したうえで，TNFレセプターIや抗TNF中和抗体に対するアフィニティー・バイオパンニングを行い，これら構造変異TNF-αの諸機能を高速解析することによって得られたものである．本方法を駆使することにより現在までに，レセプター指向性（選択性）や体内安定性に優れた機能性人工TNF-αも多数得ており，TNF-α以外の種々レセプター蛋白質や抗体についても，活性を保持したリジン欠損体などを数多く得ている．したがって本研究で確立した「ファージ表面提示法を駆使した機能性人工蛋白質の創製システム」は，"プロテオーム創薬のための競争力（DDS基盤テクノロジー）"を提供するだけでなく，従来までの点突然変異法（アラニン・スキャン）では得られなかった"蛋白改変の概念"や"蛋白質の構造-活性相関概念"をも新たに提唱するものである.

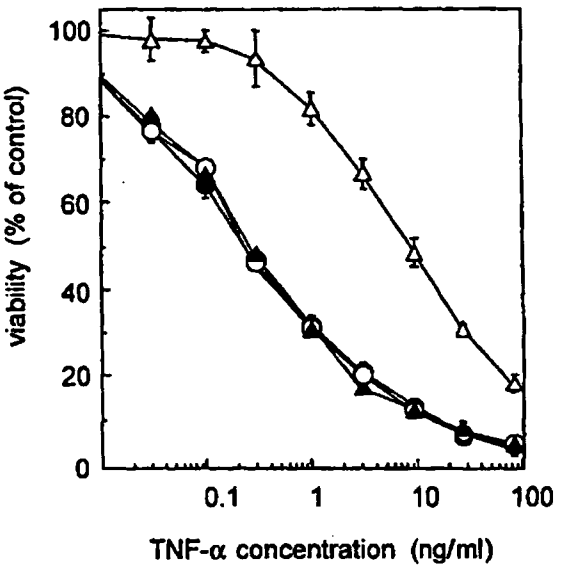

Fig. 3. *In vitro* Bioactivity of Mono-PEGylated TNF-αs
The specific activity of TNF-αs was measured by a cytotoxicity assay using L-M cells in the presence of actinomycin D. Each data value represents the mean±S.D. ○: wTNF-α, □: ran-PEG-TNF-α (randomly mono-PEGylated wTNF-α with linear-type PEG5000, ●: mTNF-α-Lys(-), ▲: sp-PEG-mTNF-α (*N*-terminus specific mono-PEGylated mTNF-α-Lys(−)).

プロテオーム創薬は，疾患プロテオミクス及び構造ゲノミクスなどの進展と，これらの知見を統括したバイオインフォマティクスが駆動力となり，近い将来，上記の「医薬価値に優れた機能性人工蛋白質を迅速創製できる蛋白質分子進化戦略」との融合により加速度的に推進されるものと期待される．一方でこのようなプロテオーム創薬を指向したバイオインフォマティクスの進展は，蛋白質のアミノ酸配列と立体構造，機能との連関を理解可能とするため，近未来的にはアミノ酸配列が与えられれば，その配列から未知蛋白質の構造と機能が予測し得よう．こ